

**“RELATIONSHIP BETWEEN SATELLITE-DERIVED AEROSOL
OPTICAL DEPTH AND GROUND LEVEL PM₁₀
CONCENTRATIONS AT SHIMLA”**

A Thesis

*Submitted in partial fulfillment of the requirements for the award of the degree
of*

MASTER OF TECHNOLOGY

IN

CIVIL ENGINEERING

With specialization in

ENVIRONMENTAL ENGINEERING

Under the supervision of

Dr. Rajiv Ganguly
(Associate Professor)

By

Guru Sharan Dass Sharma
(142751)

to



JAYPEE UNIVERSITY OF INFORMATION TECHNOLOGY

WAKNAGHAT, SOLAN – 173 234

HIMACHAL PRADESH, INDIA

August-2016

CERTIFICATE

This is to certify that the work which is being presented in the thesis titled “**Relationship between Satellite-Derived Aerosol Optical Depth and Ground Level PM₁₀- concentrations at Shimla**” in partial fulfillment of the requirements for the award of the degree of Master of Technology in Civil Engineering with specialization in “**Environmental Engineering**” and submitted to the Department of Civil Engineering, Jaypee University of Information Technology, Wagnaghat is an authentic record of work carried out by **Guru Sharan Dass Sharma (Enrolment No. 142751)** during a period from July 2015 to June 2016 under the supervision of **Dr. Rajiv Ganguly** Associate Professor, Department of Civil Engineering, Jaypee University of Information Technology, Wagnaghat.

The above statement made is correct to the best of our knowledge.

Date: -

Dr. Ashok Kumar Gupta
Professor & Head of Department
Department of Civil Engineering
JUIT Wagnaghat

Dr. Rajiv Ganguly
Associate Professor
Department of Civil Engineering
JUIT Wagnaghat

ACKNOWLEDGEMENT

First of all, I would like to express deep gratitude to my project guide **Dr. Rajiv Ganguly**, (*Associate Professor, Department of Civil Engineering*) for providing me an opportunity to work under his supervision and guidance. He has always been our motivation for carrying out the project. Their constant encouragement at every step was a precious asset during work.

I express deep appreciation and sincere thanks to **Prof. Ashok Kumar Gupta** , Head of the Civil Engineering Department for providing all kinds of possible help and encouragement during project work.

I am also thankful to the faculty of Department of Civil Engineering, Jaypee University of Information Technology for providing all facilities required for the experimental work.

I am also thankful to the faculty of Department of Himachal Pradesh Pollution Control Board for providing the required data for the analysis work.

My special thanks to my classmates & friends who gave me memorable moments during this course.

Finally I am highly thankful to my parents for inspiring me and fulfill my all wishes.

ABSTRACT

Aerosols are a fundamental component of Earth's atmospheric chemistry and radiative balance. Atmospheric aerosols can affect climate through the Earth's radiation balance by scattering and absorbing incoming solar radiation and by acting cloud condensation nuclei.

Atmospheric aerosols play an important role in the understanding of global and regional climate effects. Knowledge of aerosol properties is essential for correcting the atmospheric effect in satellite remote sensing of Earth's surface. Therefore, the understanding of aerosol and their radiative effects are important in climate forcing studies.

To assess the relationship of ground-level fine particulate matter (PM) the concentrations measured as part of the National Ambient air quality monitoring (NAAQM) network at two monitoring stations in Shimla city, versus remote-sensed PM_{10} determined from aerosol optical depth (AOD) calculated by the Moderate Resolution Imaging Spectroradiometer (MODIS) satellite instruments. The Shimla city in Himachal Pradesh has air quality trouble directly attributed to particulate matter in India primarily due to vehicular emissions. State and Central regulatory agencies monitor particulate matter with a network of ground sensors throughout the Shimla. Satellite technology provides aerosol optical depth data for the entire world every two days. Varying degrees of correlation have been found worldwide in the research of comparing satellite aerosol optical depth to ground sensor particulate matter. The satellite and ground data were compared on the basis of the linear correlation (R), standard deviation (SD), index of agreement (IA), normalized mean square error (NMSE), Pearson's correlation coefficient (R), the fractional bias (FB) and the factor of two (F^2). In Shimla comparing PM_{10} data to satellite aerosol optical depth data demonstrates a varying correlation seasonally.

Keywords: Particulate Matter (PM_{10}), Moderate Resolution Imaging Spectroradiometer (MODIS), Aerosol Optical Depth (AOD), GeoTIFF, HDF.

TABLE OF CONTENTS

CERTIFICATE	I
ACKNOWLEDGEMENT	II
ABSTRACT	III
TABLE OF CONTENT	IV
LIST OF FIGURES	VII
LIST OF TABLES	IX
LIST OF ACRONYMS	X

Contents

LIST OF FIGURES

LIST OF TABLES

LIST OF ACRONYMS

AERONET	Aerosol Robotic Network
AOD	Aerosol Optical Depth
HPPCB	Himachal Pradesh Pollution Control Board
EPA	United States Environmental Protection Agency
GeoTIFF	Geographically Referenced Tagged Image File Format
GIS	Geographic Information Systems
HEG	HDF EOS to GeoTIFF
LIDAR	Light Detection and Ranging
MISR	Multi-angle Imaging SpectroRadiometer
MODIS	Moderate Resolution Imaging Spectroradiometer
NASA	National Aeronautic and Space Administration
PM	Particulate Matter
NAAQS	National Ambient Air Quality Standard
NAMP	National Air Quality Monitoring Programme
RSPM	Respirable Suspended Particulate Matter

Chapter 1

Introduction

1.1 General Introduction

Particulate matter (PM) is the general term utilized for a blend of strong particles and fluid beads found in the climate. Observing characteristic (dust and volcanic fiery remains) and anthropogenic aerosols (biomass blazing smoke, mechanical contamination) has increased renewed consideration since they impact cloud properties, modify the radiation spending plan of the earth-environment framework, influence barometrical dissemination examples and cause changes in surface temperature and precipitation. Aerosols likewise lessen perceivability and incite respiratory ailments when sub-micron measured aerosols infiltrate the lungs consequently influencing air quality and wellbeing of humans. Expanded presentation to particulate matter with streamlined diameters 1 less than $10\mu\text{m}$ (PM_{10}) can bring about lung and respiratory maladies and even unexpected death (Martin et.al. 2008).

The extraction of aerosol optical thickness (AOT) gives a way to the appraisal of air contamination, as the key parameter for surveying climatic or air contamination in photochemical air contamination studies is the AOT. As well, AOD is likewise the most critical obscure of each air remedy calculation for sorting out the radiative transfer (RT) condition and expelling environmental impacts from satellite remotely detected pictures utilizing air adjustment. In this manner, the AOD got from the barometrical way brilliance has been utilized as a device of evaluating environmental contamination.

The primary source of development of aerosols (particulates) is from discharges of gasses mostly because of man-made and natural sources. Many analysts have analyzed the relationship amongst AOD and particulate matter (Chu et.al 2006). The relationship amongst AOD and PM_{10} or $\text{PM}_{2.5}$ can be utilized to change over the satellite estimations to air quality records. While

satellites can give solid, repeated and concise estimations from space, examination with observing surface level air contamination keeps on being a test since satellite estimations are column-integrated quantities.

1.2 Physical and chemical characteristics of aerosols

The chemical properties, physical properties, lifetimes and plenitudes are the variables on which natural effects of atmospheric particles depend on. The size circulation, focus and piece of atmospheric aerosol particles measure greatly variable each transiently and spatially.

1.2.1 Concentrations

Different measures are commonly used to describe the aerosol concentration: these are number, area volume and mass concentrations.

Table 1 Commonly used measures of aerosol concentration (Heintzenber, 2004)

Name	Unit	Description
Number concentration	cm^{-3}	N
Area concentration	$\mu\text{m}^2 \text{cm}^{-3}$	$4 r^2 \pi N$
Volume concentration	$\mu\text{m}^3 \text{cm}^{-3}$	$4/3 r^3 \pi N$
Mass concentration	$\mu\text{g m}^{-3}$	$4/3 r^3 \pi N \rho$

Table 2 Number concentration and mass concentration of aerosol particles at different locations. (Heintzenber, 2004)

Location	Number concentration (cm^{-3})	Mass concentration ($\mu\text{g m}^{-3}$)
Urban	$10^5 - 10^7$	$10^1 - 10^4$
Rural	$10^3 - 10^4$	$10^1 - 10^2$
Remote maritime	10^2	$10^1 - 10^2$
Polar	$10^0 - 10^3$	$10^{-1} - 10^1$

In the lower troposphere, the particle number concentration ordinarily fluctuates in the scope of around $10^2 - 10^5 \text{ cm}^{-3}$, and run of the mill mass fixation shifts somewhere around 1 and $100 \mu\text{g m}^{-3}$ (Table 2) Aerosol concentrations in the free troposphere are normally 1–2 order of size lower than in the atmospheric limit layer.

PM_x (particulate matter with diameter not as much as X) is additionally used to depict the aerosol mass fixation.

1.2.2 Size distribution:

Aerosol particles in the climate have generally variable shapes. Their measurements are generally portrayed by a molecule breadth, which range more than four orders of size, from a couple of nanometers to around 100 μm . Molecule size is a standout amongst the most imperative parameters to portray the conduct of aerosols, influencing both their lifetime, physical and chemical properties. Dissemination of aerosol particles is for the most part characterized by their number, surface area or volume. (Figure 1)

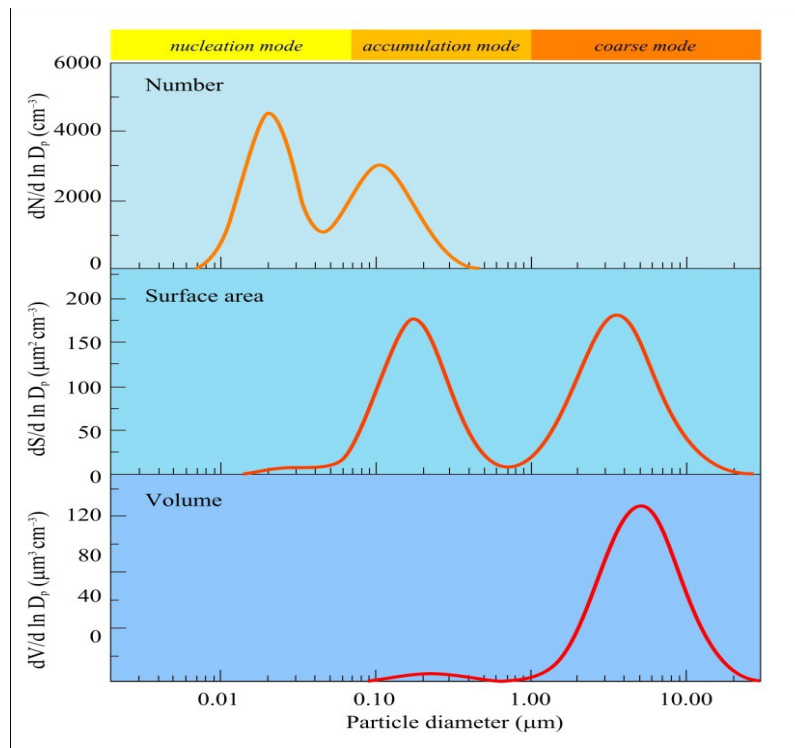


Figure 1 Number, surface and volume distributions of aerosol particles. The areas below the curves correspond to the total aerosol number, surface and volume, respectively. (Heintzenber, 2004)

Based on particle distributions, different groups of atmospheric particles can be separated:

- Nucleation (Aitken) mode (particle diameter $< 0.1 \mu\text{m}$),
- Accumulation mode (particle diameter: $0.1 \mu\text{m} > d > 1 \mu\text{m}$),
- Coarse mode (particle diameter $d > 1 \mu\text{m}$).

Aerosol particles underneath $0.1 \mu\text{m}$ in distance across constitute the nucleation (or Aitken) mode. The littlest scope of these particles (with molecule breadth is lower than $0.01 \mu\text{m}$) once in a while called ultrafine mode. These particles are formed by homogeneous and heterogeneous nucleation forms (Figure 2). They can shape amid common gas-to molecule buildup (Figure 3)

or amid buildup of hot vapor in burning procedures. Because of their fast coagulation (Figure 4) or arbitrary impaction onto surfaces, the lifetime of these little particles is short (less than an hour).

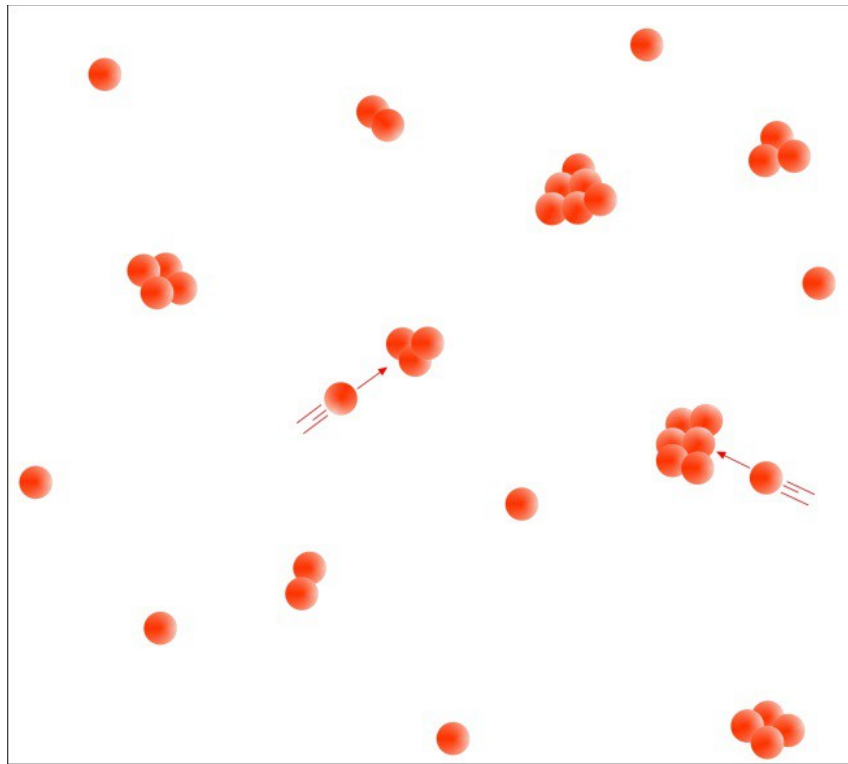


Figure 2 Homogeneous nucleation of aerosol particles (Heintzenber, 2004)

Bigger airborne particles in the size reach 0.1 to 1 μm in distance across can aggregate in the environment on the grounds that their evacuation systems are minimum effective. Their lifetime in the environment is 7–10 days and amid this period they can transported to a long separation from their sources. Particles having a place with this collection mode are shaped predominantly by coagulation (Figure 3) of littler particles or buildup of vapors onto existing particles, and amid these components they develop into this size extent.

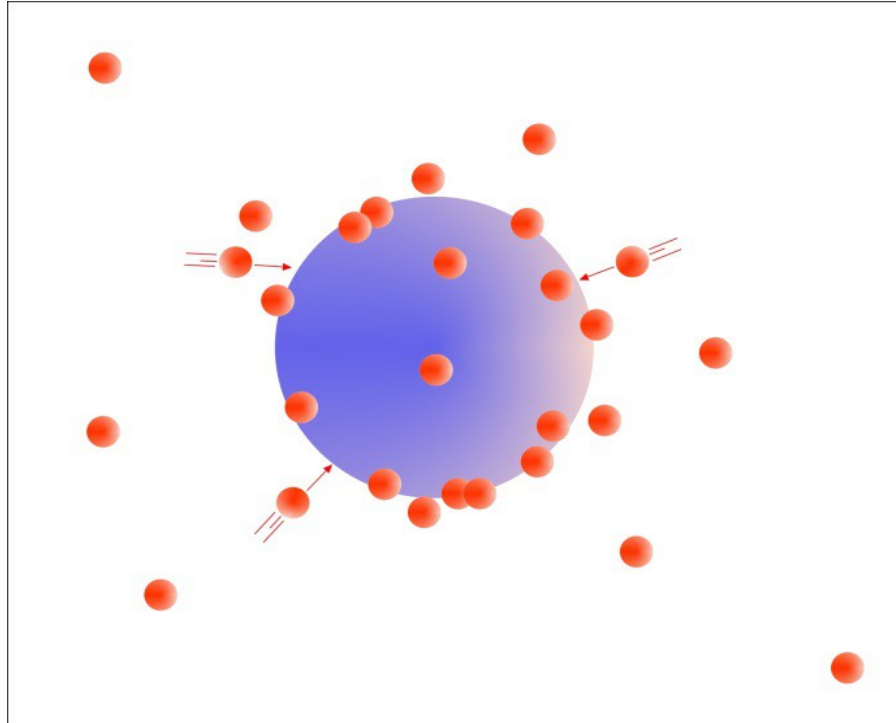


Figure 3 Condensation of aerosol particles(Heintzenber, 2004

In the meantime, they can likewise be discharged to the environment from various sources, for the most part from fragmented combustion. Aggregation particles expelled from the climate predominantly by wet deposition.

The Coarse mode have particles with diameter bigger than $1.0 \mu\text{m}$. These particles for the most part transmitted to the climate amid mechanical procedures from both natural and manmade sources (e.g. ocean salt particles from sea surface, soil and mineral dust, organic materials). Because of their generally large mass, they have less atmospheric lifetimes in view of their fast sedimentation.

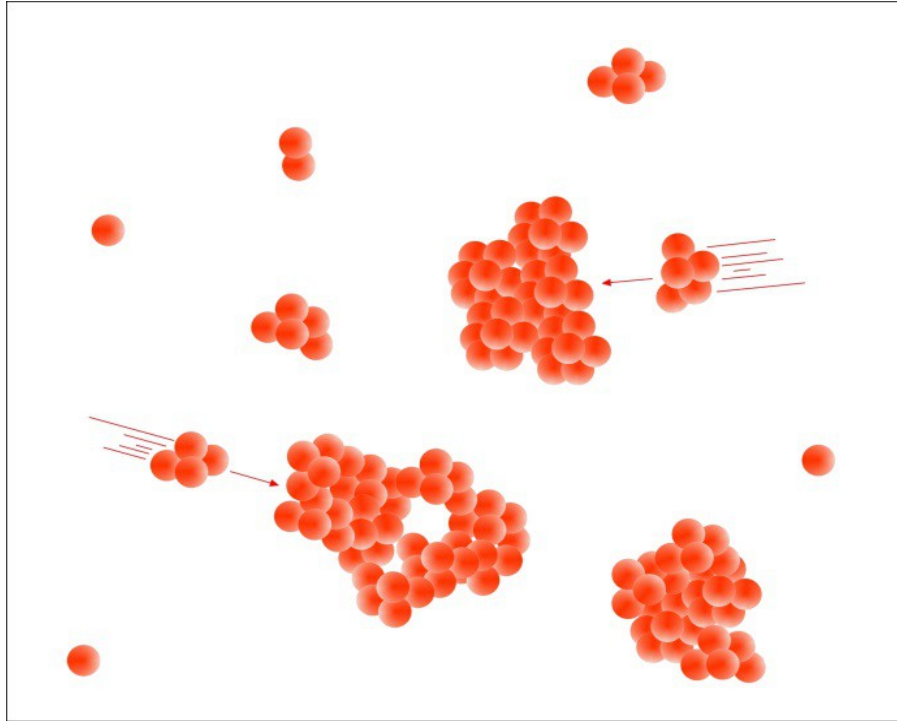


Figure 4 Coagulation of aerosol particles (Heintzenber, 2004)

The conveyance of atmospheric aerosol particles can be found in Figure 1. Little particles in nucleation mode constitute the greater part of atmospheric particles by number. However because of their little sizes, their commitment to the aggregate mass of aerosols are little (around a few percent) and the Accumulation mode particles have the greatest surface area (Tsai et.al.2011). The mass or volume fixation is overwhelmed by the aerosols in coarse and aggregation modes. Size, area and volume distributions of aerosol particles show characteristic pattern at different locations (e.g. urban, rural, remote continental or marine regions). (Kaufman et.al 2003)

1.2.3 Chemical composition

The atmospheric aerosol has an exceptionally unpredictable and variable chemical organization. Because of the different sources and changes, every molecule has character arrangement. (Mao et.al 2011) Atmospheric aerosols are for the most part made out of variable measures of sulfate, nitrate, ammonium, sea salt, crustal components and carbonaceous mixes

(elemental and organic carbon) and other natural materials (Mao et.al 2011). Fine particles prevalently contain sulfate, nitrate, ammonium, natural and natural carbon and certain follow metals (e.g. lead, cadmium, nickel, copper and so on.). The essential segments of coarse molecule portion are dust, crustal components, nitrate, sodium, chloride and biogenic natural particles (e.g. dust, spores, plant sections etc.).

The main reasons of sulphate component (SO_4^{2-}) in the troposphere are sulphur dioxide (SO_2) discharged from artificial sources and volcanoes, and dimethyl sulphide (DMS) from biogenic sources, especially from marine planktons. In the stratosphere, sulphate aerosols generally changed from carbonyl sulphide (COS). (Mao et.al 2011)

Nitrate (NO_3^-) is formed primarily from the oxidation of atmospheric nitrogen dioxide (NO_2). Ammonium salts are also common components of atmospheric aerosols. They are formed through the reactions among ammonia (NH_3) and various acids, like sulphuric (H_2SO_4) and nitric acids (HNO_3). When atmospheric ammonia neutralizes these acids, ammonium sulphate ($(\text{NH}_4)_2\text{SO}_4$), and ammonium nitrate (NH_4NO_3) particles are formed. Main source of chloride (Cl^-) is sea spray, but ammonium chloride (NH_4Cl) particles form also during the interaction between ammonia and hydrochloric acid (HCl) (Schaap et.al 2009). These aerosols are also known as sea sprays.

Carbonaceous materials constitute an extensive but very variable portion of the air aerosol. The carbonaceous division of the aerosols comprises of both Organic carbon (OC) and Black carbon (BC) or Elemental carbon (EC). The proportion of natural to aggregate carbon (EC+OC) is unequivocally relies on upon the sources (Schaap et.al 2009). The fundamental sources of essential carbon particles are biomass and fossil fuel usage. Particles containing natural carbon can discharged specifically to the environment additionally from biomass ignition forms and by secondary organic aerosol (SOA) arrangement amid the air oxidation of biogenic or anthropogenic volatile organic compounds (VOC) (Schaap et.al 2009).

Regular chemical arrangement of aerosols can fluctuate at various areas, times, climate conditions and molecule size parts. Figure 5, Figure 6 and Figure 7 demonstrate the relative plenitude of various chemical segments of fine particles in various areas, in urban region, in rural district and in remote sites.

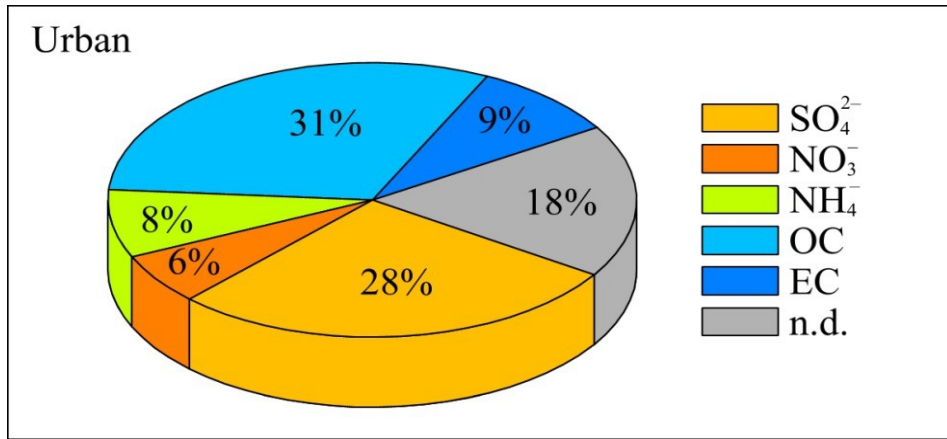


Figure 5 Average particle composition of aerosol types in urban area. (Heintzenber, 2004)

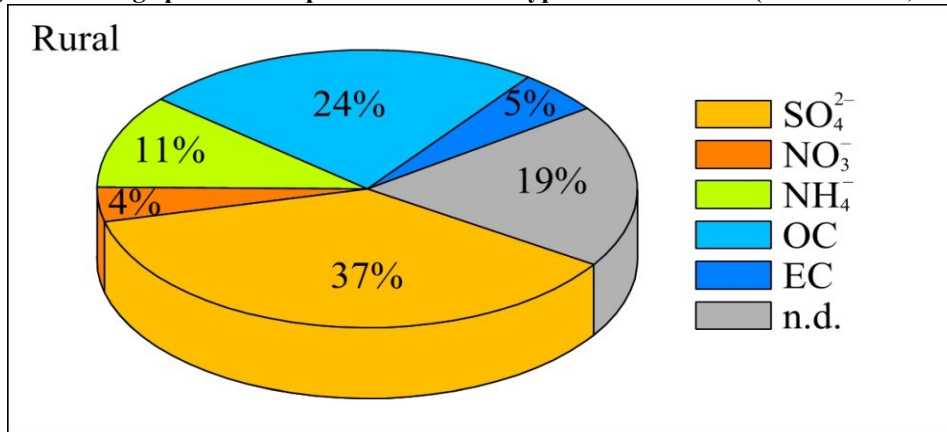


Figure 6 Average particle composition of aerosol types in rural continental region. (Heintzenber, 2004)

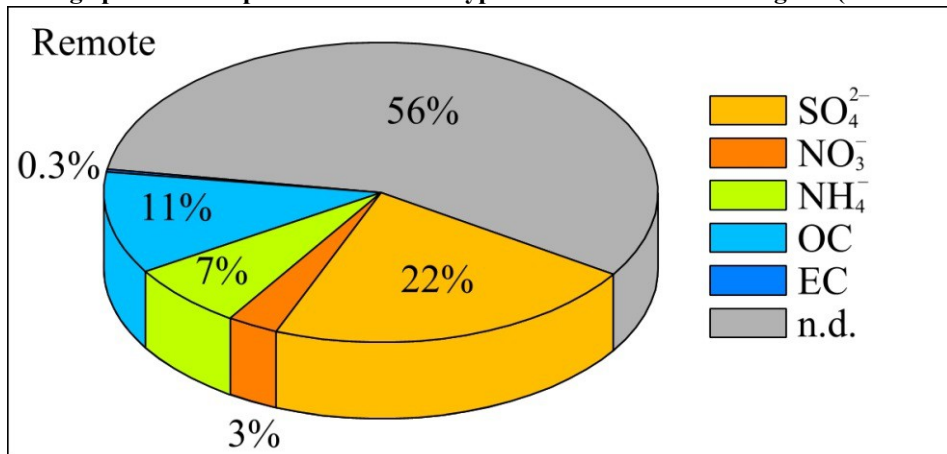


Figure 7 Average particle composition of aerosol types in remote region. (Heintzenber, 2004)

Data correspond to mass fraction in % of the total fine particle mass concentration. OC = organic carbon, EC = elementary carbon.

1.2.4 Water solubility

Atmospheric particles can likewise be arranged by their water solvency, that is, the means by which well they disintegrate in water. In mainland districts, around 80% of littler particles are water-dissolvable. Notwithstanding, a few sorts of coarse particles are additionally water dissolvable, similar to sea salt particles over seas. Most water-solvent aerosol segments are hygroscopic and they can assimilate water. In the event that aerosol particles comprising of water-solvent material, the uptake of atmospheric water vapor can results a watery arrangement bead. Amid this procedure, the measure of molecule increments by hygroscopic development, even though when relative moistness is lower than 100%(Chinnam et.al 2006). Exceptionally solvent particles are for instance ammonium sulfate, ammonium nitrate and sodium chloride. These particles are effective cloud buildup cores (CCN).

A few particles are inadequately soluble or insoluble in water. Insoluble aerosols for instance particles got from soil dust or volcanoes (e.g. metal oxides, silicates, dirt minerals). (Chinnam et.al 2006)

1.2.5 Atmospheric lifetime

The lifetime of atmospheric aerosol particles relies on upon their characterisitcs (size, chemical structure, and so on.) and on elevation range, as well (Figure 8) (Heintzenber, 2004). In the atmospheric limit layer (lower troposphere), the living arrangement time of aerosol particles is normally not more than a week, frequently on the order of a day, subjected upon aerosol properties and meteorological conditions. In the free troposphere, the molecule lifetime is 3–10 days all things considered (Heintzenber, 2004). in the midst of this time, chemical can be transported to a long distance. Accordingly, there is a huge variability in molecule concentration, geographical distribution, reflection of sources and sinks. The stratosphere additionally contains aerosol particles, which have any longer lifetime (up to 1 year), than in the tropospheric particles, because of the absence of precipitation. (Engel-Cox et.al 2004)

Smaller particles are productively evacuated by coagulation with different particles. Along these lines, their lifetime is short (in a scope of ten minutes to day). Additionally, the vast particles invest just a short energy in the climate because of the sedimentation (Heintzenber,

2004). Particles in the amassing mode have the longest lifetime (7–10 days by and large), as in this reach, both the Brownian dispersion and sedimentation are less vital. These particles expelled from the climate dominantly by wet deposition(Engel-Cox et.al 2004).

The impact of aerosols on precipitation can be sorted as takes after (Lau et al., 2008):

1. Aerosol direct impact – Aerosols disperse and/or retain sunlight based radiation, along these lines cooling the world's surface which is known as immediate impact. The lessening of solar radiation at the surface is alluded to as the solar dimming effect.

2. Aerosol semi-direct impact - Because of the nearness of aerosols, earth's surface cools more than the environment above it, the surface cooling may settle the lower troposphere, accordingly restricting convection, known as the semi-direct impact.

3. First indirect impact – Aerosol can influence the water spin through the communication with the cloud microphysical forms, whereby aerosol expands the quantity of cloud buildup cores, framing littler water beads that expansions dispersing cross segments, lights up mists, and reflects more sun oriented radiation.

4. Second indirect impact – The little beads shaping as a consequence of the main backhanded impact can confine crash and mixture, drawing out the lifetime of mists and repressing the development of cloud drops to rain drops.

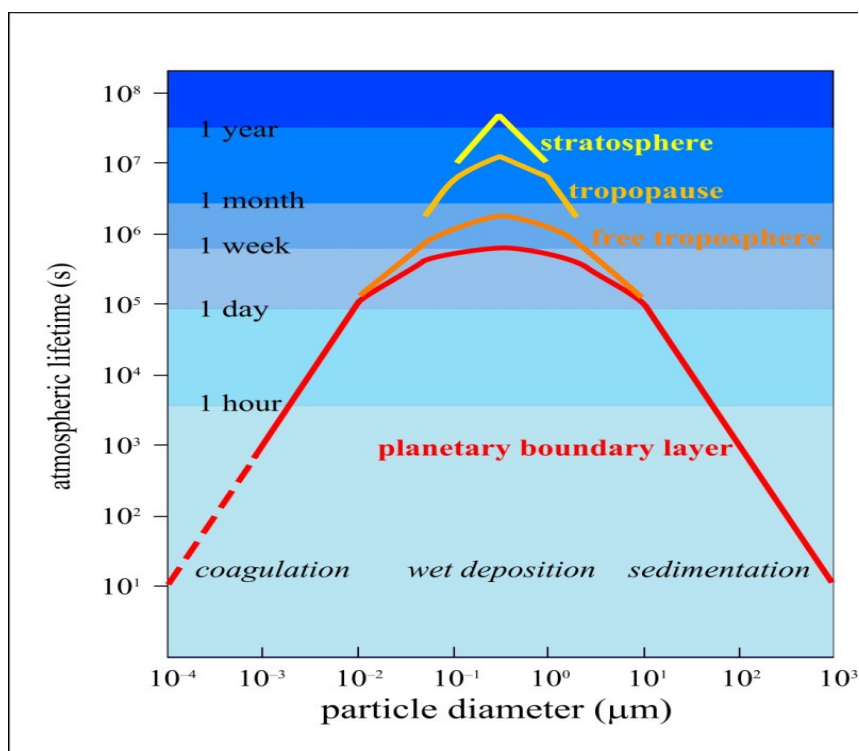


Figure 8 Atmospheric lifetime of different size particles at different levels of the atmosphere (Jaenicke, 1980)

Table 3 Main properties of different aerosol particles (Wilson and Suh, 1997):

	Nucleation mode (Fine particles)	Accumulation mode (Coarse particles)	Coarse mode (Coarse particles)
Size	$d < 0.1 \mu\text{m}$	$0.1 \mu\text{m} > d > 1 \mu\text{m}$	$d > 0.1 \mu\text{m}$
Sources	Combustion Gas-to Particle conversion Chemical reactions	Combustion Gas-to Particle conversion Chemical reactions	Dust Soil Biological sources Sea spray
Formation	Chemical reactions Nucleation Condensation Coagulation	Nucleation Condensation Coagulation Evaporation of droplet	Mechanical disruption of surface Suspension of dust Evaporation of sea spray Chemical reactions
Composition	Sulphate Elemental carbon Trace metals, Low-volatility organic compounds	Sulphate Nitrate Ammonium Elemental Carbon Organic Component Trace metals (Pb, Cd, V, Ni, Cu, Zn, Fe, etc.)	Dust Ash Crustal elements Sea salt Nitrate Biogenic organic particles
Solubility	Largely soluble, hygroscopic	Largely soluble, hygroscopic	Largely insoluble, non- hygroscopic

Travel distance	<a few 10 of km	a few 100 to 1000 of km	<a few 10 of km (sometimes larger)
Typical atmospheric lifetime	Minutes to hours	Days to weeks	Minutes to days
Sinks	Growth into accumulation mode, wet and dry deposition	Wet deposition, dry deposition (Brownian diffusion, turbulence)	Wet deposition, Dry deposition (sedimentation, turbulence)

1.3 Aerosol Optical Thickness – Aerosol Optical Depth (AOD)

The key parameter for evaluating atmospheric contamination in air pollution studies is the aerosol optical thickness, which is likewise the most critical obscure component of each atmospheric amendment calculation for comprehending the radiative transfer equation and expelling atmospheric impacts from satellite remotely detected pictures (Hadjimitsis et al, 2004). Aerosol optical thickness (AOT) is a measure of aerosol stacking in the environment (Retails et al, 2010). High AOT values recommend high convergence of aerosols, and along these lines air contamination (Retalis et al, 2010). The utilization of earth perception depends on the checking and determination of AOT either immediate or aberrant as apparatus for surveying and measure air pollution (Hadjimitsis et al, 2004). Estimations on PM_{2.5} and PM₁₀ are observed to be connected with the AOT values as appeared by Lee et al. (2011), Hadjimitsis et al. (2010), Nisantzi et al. (2011). "Aerosol Optical Thickness" is characterized as the extent to which aerosols keep the transmission of light. The aerosol optical depth or optical thickness (τ) is characterized as 'the coordinated annihilation coefficient over a vertical segment of unit cross area. Termination coefficient is the fragmentary consumption of brilliance per unit way length additionally called weakening particularly in reference to radar frequencies.

(http://daac.gsfc.nasa.gov/dataholdings/PIP/aerosol_optical_thickness_or_depth.shtml).

1.3.1 Calculating Aerosol Optical Thickness

The force I of a light beam emission of a specific wavelength that achieves Earth's surface is given by

$$I = I_0 e^{-(am)}$$

Where I_0 is the intensity of daylight simply over Earth's environment, a is the aggregate atmospheric optical thickness, and m is the relative air mass. $m=1$ when the sun is

straightforwardly overhead and is generally around equivalent to $\sec(z)$, where z is the sun oriented pinnacle point.

The sun powered pinnacle edge is the edge between the apex and the focal point of the sun's circle. The sun based height point is the elevation of the sun, the edge between the skyline and the focal point of the sun's circle.

The aggregate atmospheric optical thickness can be separated into two sections, one section because of the way that atoms in the climate disperse light out of an immediate pillar from the sun (Rayleigh dissipating) and another part because of disseminating by aerosols. The Rayleigh dispersing term a_R is corresponding to the proportion of atmospheric weight at the eyewitness' area to sea level atmospheric weight, p/p_o . Subsequently,

$$a = a_a + a_R(p/p_o)$$

In the event that a sun photometer measures light force such that the voltage signal delivered by the instrument is specifically relative to intensity, then

$$V = V_o(r_o/r)^2 e^{-(a_a + a_R(p/p_o))m}$$

Solving for a_a ,

$$a_a = (\ln(V_o(r_o/r)^2) - \ln(V) - a_R(p/p_o)m)/m$$

Two quantities on the right half of this condition are steady since they are properties of instrument. The voltage V_o , the extraterrestrial steady, is the voltage sun photometer record if pointed at the sun simply outside the world's atmosphere when the earth is 1 astronomical unit (AU) from the sun. The Rayleigh disseminating term a_R relies on upon the wavelength at which a specific sun photometer reacts to daylight. On account of the GLOBE sun photometer, the estimation of a_R is resolved from the ghostly reaction of the LED identifiers and is equivalent to around 0.138 for the green channel and around 0.058 for the red channel.

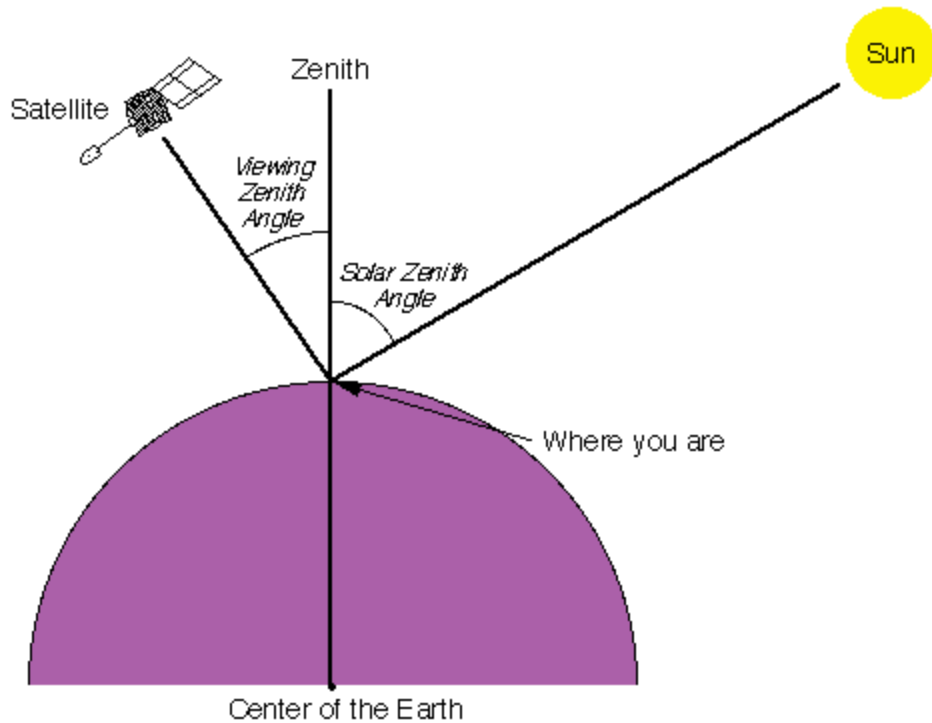


Figure 9 Schematic illustration of the Solar Zenith Angle (SZA) and Viewing Zenith Angle (VZA) for observations from satellite-based instrument. (Source NASA)

Alternate quantities on the right half of the condition rely on upon the conditions under which measurements are taken. The voltage V is recorded when the GLOBE sun photometer is pointed at the sun, short the dim voltage. The proportion r_0/r is the proportion of 1AU to the genuine separation from the earth to the sun, in units of AU, at the time you make an estimation; it is an element of the date on which an estimation is made and it is utilized to amend the steady V_0 to the voltage of sun photometer at the season of an estimation. It can decide p/p_0 either directly, with a gauge, or by indirectly (to sensible exactness) by knowing the rise of watching site.

1.4 Particulate Matter

The EPA groups "particulate matter, (PM)" (otherwise called aerosols or particle contamination), as an unpredictable blend of to a great degree fine particles and fluid beads. PM_{10} is 10 microns in diameter across additionally called "inhalable coarse particles" and $PM_{2.5}$ is 2.5 micron in diameter likewise called "fine particles" which can be effortlessly breathed in bringing on wellbeing inconvenience in the lungs and heart (EPA,2007).

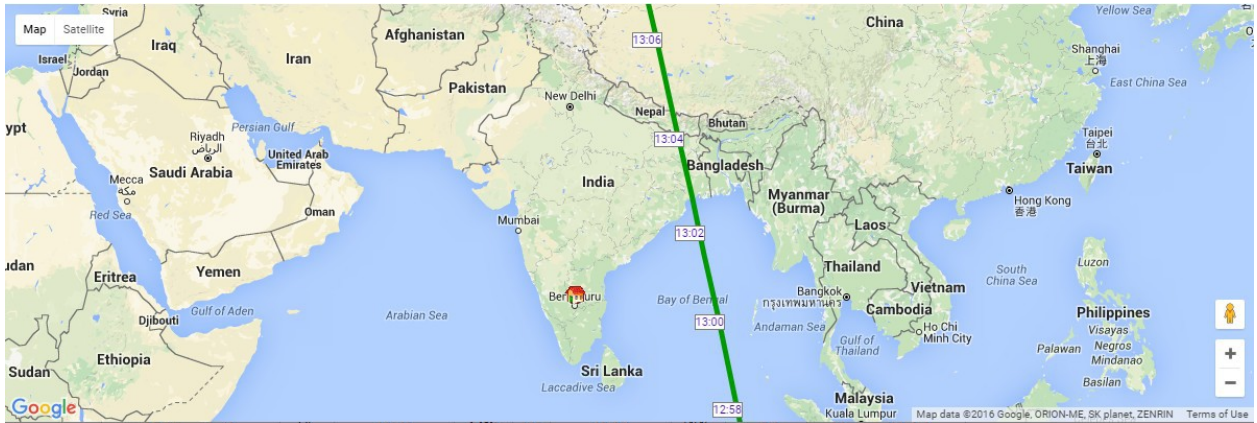


Figure 10 Satellite (Aqua) passing time over India.(Source <http://www.n2yo.com/?s=25994>)

PM is a noteworthy concern in general public wellbeing, due to the ease with which the particles can be breathed in and cause health issues. The source of the PM range from earth streets, development sites, smokestacks, fires, to the numerous substances in our atmosphere from different vehicle and modern outflows. Particulate matter incorporates various segments, including acids, (for example, nitrates and sulfates), natural chemicals, metals, and soil or dirt particles (EPA, 2007).

Particulate matter is the reason for lessened perceivability or dimness in our neighborhoods and our national parks. Particulate matter additionally impacts territorial atmosphere by changing cloud properties, stifling precipitation and engrossing solar energy.

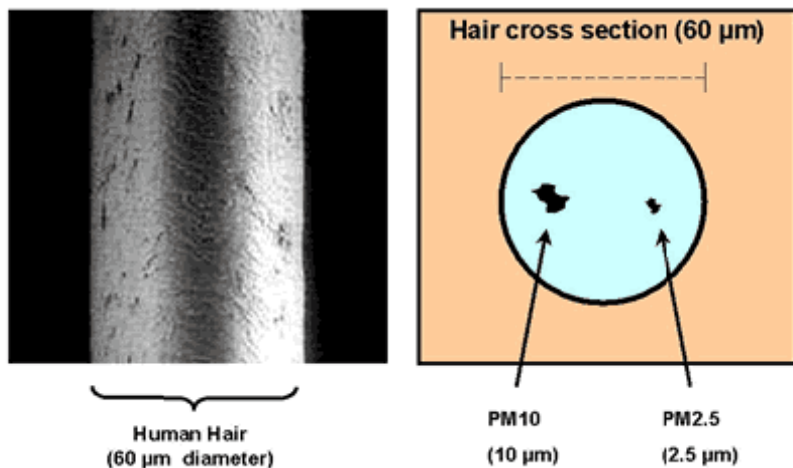


Figure 11 A size comparison of fine particulate matter

1.5 Objectives of the project work

- Arrangement of data from MODIS aqua and MODIS terra satellite database.
- Ground level PM₁₀ concentrations of study area.
- To determine the dataset's that are useful for the cities PM₁₀ calculation.
- To develop regression line and other modes of data comparison for the different data sets.
- To determine the sources of particulate matter to atmosphere in city.
- Estimating ground-level PM₁₀ with aerosol optical depth determined from satellite remote sensing.

1.6 Scope of the Project work

The project will enable the application of remote sensing thru MODIS satellite in the Himalayan region. As the instruments to monitor the particulate matter are expensive, it can be used to monitor the ground level concentrations using aerosol optical depth (AOD) aerosol optical thickness (AOT) retrieved from the MODIS and MISR instrument on board aqua and terra satellites with very genuine degree of error.

1.7 Layout of the Project work

The thesis is divided into 6 chapters:

Chapter One Includes introduction to the problem considered, and objectives of the research.

Chapter Two Consists of Theoretical background and review of literature for the study of aerosols using remote sensing and method of comparison of Satellite data measurements to ground PM₁₀. Details of some important studies also have been described.

Chapter Three Describes the extent of area of study i.e. Shimla and its topography, climate and seasons. Detailed information on the properties and characteristics of remote sensors i.e. MODIS and MISR are described along with data extraction methods and location of monitoring stations is also described

Chapter Four The chapter shows the Data analysis of the data sets for annual and seasonal relation of Aerosol optical depth to particulate matter using different statistical parameters and their significance as results.

Chapter Five The chapter includes discussion on the outcome of the thesis. Including necessary reasons for results obtained.

Chapter Six Concludes the study as AOD values showed good correlation with the ground measurements AOD studies can be used for predicting the PM₁₀ concentrations in the city.

Chapter 2

Literature review

2.1 General

A complete survey of writing on aerosol optical depth and particulate matter relationship are consolidated in this section. The section examines the diverse AOD sensors advances, distinctive systems for the upgrade of AOD utility and different trial contemplates on utilization of remote sensing for Particulate fixations.

Particulate matter is a complex blend of tiny solids and fluid beads suspended all around that comprises of various segments including: nitrates and sulfates, metals, soil and dirt particles, natural chemicals, pieces of dust and form spores, water, residue, smoke and tire elastic.

Fine particulate matter can be specifically transmitted or framed by auxiliary chemical reactions in the atmosphere. Sulfur dioxide, for instance, is particle formed from industrial facilities and power plants. Nitrates are framed in a comparative style from nitrogen oxides discharged from power plants, cars and different sources of burning (EPA 2013c).

The EPA a while later evaluated the first measures in 1979 and executed changes by 1987, when the essential pointer of particles was changed from TSP to PM₁₀, completely outlining particles sufficiently small to infiltrate further into the respiratory tract (thoracic particles) and along these lines more inclined to antagonistically influence public wellbeing. The new essential standard for PM₁₀ was not to surpass 150µg/m³ more than once per year and with a yearly mean of 50µg/m³ (EPA 2013d).

A second survey started in 1994 that prompted fine particulate matter 10µg or smaller assigned as a tactful classification subject to regulation control. The choice depended on studies that related fine particles with genuine health impacts (Pope 1995; Laden et al. 2000; Harrison and Yin 2000; Schlesinger 2007; van Donkelaar et al. 2010). Gauges for PM₁₀ were set at

15 $\mu\text{g}/\text{m}^3$ (yearly mean) and 65 $\mu\text{g}/\text{m}^3$ (24-hour normal). The guidelines for PM₁₀ were kept up at the past levels set in 1987. The new controls, which produced results in 1997, were tested in court by a few associations, enterprises, and state governments. The U.S. Preeminent Court at last maintained the new principles by a consistent choice in 2001 insisting the EPA's power to control air quality under the Clean Air Act and decided that expense can't be considered in setting models. The EPA further fixed PM₁₀ principles in 2006, lessening the 24-hour levels to 35 $\mu\text{g}/\text{m}^3$ from 65 $\mu\text{g}/\text{m}^3$ and again in 2012 when the yearly mean standard was brought down to $\mu\text{g}/\text{m}^3$. The National Air Monitoring Program (NAMP) is an across the country program headed by the Central Pollution Control Board whose reason for existing is to screen levels of key air pollutants, report infringement, and behavior research on contamination patterns. NAMP screens levels of SO₂, NO₂, Suspended Particulate Matter (SPM), and Respirable Suspended Particulate Matter (RSPM/PM₁₀) at 342 working stations in 127 urban areas crosswise over India.

Table 4 Indian standards for Particulate matter

Parameter	Time Weighted Average	Industrial, Residential, Rural and Other Area	Ecologically Sensitive Area (notified by Central Government)
PM ₁₀ , $\mu\text{g}/\text{m}^3$	Annual*	60	60
	24 hours**	100	100
PM ₁₀ , $\mu\text{g}/\text{m}^3$	Annual*	40	40
	24 hours**	60	60

2.2 Remote sensing of Particulates

The utilization of satellite remote sensing to analyse atmospheric aerosols was initially utilized as a part of the 1970s. Satellite pictures are being weakened because of the retaining and diffusing impact of particles in the atmosphere and calculations were intended to amend for this distortion; in any case, it was understood that contemplating the backscatter radiation itself could uncover properties about aerosols in the atmosphere.

Table 5 degree of light extinction attributed to aerosols (Huda et.al)

AOD value	Corresponding conditions
Less than 0.5	Very clear bright blue sky

Approaching 1	Hazy
2.0-3.0	Dust storms, large fires or polluted urban areas
3.0 or above	Solar disk appears red.
8.0	Sun is not visible.

The occurrence of aerosols in an atmospheric column of air will keep a specific measure of reflected light from being transmitted to the satellite sensor. It then takes after that the optical profundity (or depth) of the atmosphere could be utilized as an intermediary for evaluating the measure of particulate matter close to the surface.

2.3 Analytical studies

Various studies have connected MODIS AOD to gauge particulate matter concentrations close to the surface (Gupta et al 2006; DiNicolantonio et al. 2009; Schapp 2009; Tian and Chen 2009; Natunen et al. 2010). While different instruments, for example, MISR, have a better spatial determination, they don't have an everyday worldwide return to time. This makes MODIS more useful from an arranging/administration position for assessing day by day particulate matter (Gupta et al 2006). A quantitative relationship was initially settled utilizing a basic straight relapse to associate AOD values with ground-based PM₁₀ estimations and their varieties over space and time (Chu et al. 1998, 2003; Engel-Cox 2004; Zhang et al. 2006; Gupta and Christopher 2008; Christopher and Gupta 2009; Li et al. 2009). All of these studies were on a worldwide or national scale and the quality of the relationships changed in light of land area. Nevertheless, the potential for applying MODIS AOD to screen and foresee contamination levels close to the surface was sufficiently promising to warrant further examinations.

Chu et al. (2003) distributed one of the primary papers to apply satellite determined AOD qualities to gauge particulate matter on a provincial and urban scale. The study zones were eastern China and India, the eastern United State/Canada and Western Europe. These locales speak to the most crowded and industrialized areas on the planet. Three urban ranges were likewise chosen: Northern Italy, Greater Los Angeles, and Beijing, China. The study had two primary destinations: to figure out whether AOD estimations from MODIS were as exact as ground based LIDAR estimations; and to examine whether AOD information was sufficiently hearty to gauge particulate matter on numerous scales. Relapse examination was utilized to

connect LIDAR determined AOD estimations with ground-based estimations of PM₁₀, and after that AOD information from MODIS were contrasted and the LIDAR inferred AOD for acceptance. Straight relapse examinations of MODIS and AOD brought about a R connection coefficient more noteworthy than 0.90, exhibiting that MODIS AOD were as strong as AOD measured by ground-based LIDAR estimations.

Chu et al. (2003) published one of the first papers to apply satellite derived AOD values to estimate particulate matter on a regional and urban scale. The study areas were eastern China and India, the eastern United State/Canada and Western Europe. These sites represent the most populous and industrialized regions on the planet. Three urban areas were also selected: Northern Italy, Greater Los Angeles, and Beijing, China. The study had two main objectives: to determine if AOD measurements from MODIS were as accurate as ground based LIDAR measurements; and to investigate whether AOD data was robust enough to estimate particulate matter on multiple scales. Regression analysis was used to correlate LIDAR derived AOD measurements with ground-based measurements of PM₁₀, and then AOD data from MODIS were compared with the LIDAR derived AOD for validation. Linear regression comparisons of MODIS and AOD resulted in an R correlation coefficient greater than 0.90, demonstrating that MODIS AOD were as robust as AOD measured by ground-based LIDAR measurements.

Chu et al. (2003) regressed ground-based LIDAR AOD with PM₁₀ ground estimations. In northern Italy, this yielded a R-estimation of 0.82, showing the capability of utilizing MODIS AOD for surveying and predicting local air quality. The era of the study was from July 2000 through May 2001. The study found a solid regular variety with AOD most extreme happening in the spring and summer and the base amid the winter. Chu et al. (2003) laid the foundation for resulting research corresponding MODIS AOD with surface PM₁₀ levels.

Zhang et al. (2006) further examined the topographical and seasonal variation in the connection amongst AOD and PM₁₀ over the coterminous United States. Two years of MODIS AOD information (2005-2006) from both the Terra and Aqua satellites were coordinated with ground-estimations from the ten EPA locales to decide the relationship amongst AOD and PM₁₀. Their outcomes demonstrated an unmistakable topographical and seasonal impact on the quality of the PM₁₀ relationship. Great results were watched for the most part over the eastern United States in summer and fall. The southeastern U.S. had the most highest relationship ($r = 0.63$, $r^2 =$

0.40) while the southwest locale, Region 9, which incorporates California, had the least connection ($r = 0.26$, $r^2 = 0.07$). No meteorological parameters were consolidated in this study.

Engel-Cox et al. (2004) thought about subjective genuine nature pictures and quantitative AOD information from MODIS with ground-based EPA observing systems to figure out whether satellite remote sensing is practical for checking urban air quality. They develop the ideas introduced in Chu et al. (2003) by consolidating MODIS inferred AOD information and ground-based $PM_{2.5}$ and PM_{10} estimations in a relapse examination. The study was on a substantial scale and joined the touching United States and had three fundamental objectives: to test how well MODIS can picture particular aerosol transport occasions; to associate AOD from MODIS with EPA ground-based estimations; and to survey the abilities and confinements of MODIS AOD information for EPA air quality observing. The era was from April 1 through September 30, 2002.

Provincial contrasts in the adequacy of AOD estimations from MODIS were distinguished. R-values extended from close to zero to as high as 0.9. Relationships were high ($>.50$) east of 100° W (Engel-Cox 2004). The relationship of ground estimations and satellite-based estimations contrast territorially. Nearby territory, climate and atmosphere examples are a portion of the elements that influence the AOD- PM_{10} relationship. All things considered, the creators reason that MODIS can be utilized to help organizations in observing air quality to meet EPA norms.

Gupta and Christopher (2008) utilized seven years of MODIS AOD information and PM_{10} ground estimations from one site in Birmingham, Alabama to assess the viability of MODIS in checking air quality and to better comprehend the month to month, occasional, and bury yearly relationship between fine particulate matter and AOD. The connection amongst AOD and PM_{10} brought about a r-value of 0.52 utilizing day by day mean PM_{10} information. The r-value expanded to 0.62 when hourly PM_{10} was utilized.

In a comparative study, Tian and Chen (2010) took a gander at the impacts of time averaging on AOD- PM_{10} relationships from MODIS over southern Ontario, Canada. Hourly, 3-hour and every day mean ground-level PM_{10} was contrasted with locate the best general connection. The 3-hour time window performed best with a r-estimation of .593. Tian and Chen additionally found that AOD values collected more than 3×3 pixels from the Terra and Aqua satellites enhanced the connection by .03 contrasted and utilizing the single focus pixel values.

Natunen et al. (2010) likewise led a multiple year investigation of the relationship amongst AOD and PM₁₀ on a smaller local scale in Finland. Information gathered somewhere around 2000 and 2006 were gotten from ground estimations of PM₁₀ at four stations in Helsinki and from MODIS AOD on the Terra and Aqua satellites to research how worldly PM₁₀ averaging and regularity influence the relationship amongst AOD and PM₁₀. They found that time averaging expanded the relationship contrasted and utilizing hourly PM₁₀. Hourly PM₁₀ was matched with the closest satellite bridge time. An extra hour on either side of the hourly estimation up to 24 hours was then arrived at the midpoint of and connected with the AOD esteem. The time normal with the most astounding relationship changed among the four destinations with the best results discovered utilizing 19, 15, 5 and 24-hour mean qualities. Month to month mean relationships extended somewhere around 0.57 and 0.91.

Ensuing exploration grew more complex observational models that consolidate ecological elements, for example, meteorology and geographic information into different relapse examinations at territorial and urban scales (Wallace and Kanaroglou 2007; Kumar et al. 2008; Li et al. 2009; Mao et al. 2011). A standout amongst the most vital ecological parameters to consider when assessing air quality from satellites is the height of the planetary boundary layer (PBL) in light of the fact that it influences the vertical allocation of aerosols. PBL is for the most part is created in the middle of the day with a solid reversal at the top. Inside this layer, anthropogenic aerosols are very much blended and bound. This is essential in light of the fact that AOD measures the aerosol extinction for the whole atmospheric section of air from the beginning to the satellite sensor. AOD estimations will be the same whether the boundary layer is all around created or not. On account of a high boundary layer with a weak reversal, ground-based estimations of PM₁₀ may not relate well with AOD values (Gupta and Christopher 2009). The AOD-PM₁₀ relationship firmly relies on upon the stature of the planetary boundary layer. This, alongside meteorological parameters like relative mugginess that influence particle development and development, is the reason straightforward two-variable regression investigations relating AOD with PM₁₀ alone are not satisfactory for evaluating ground-level PM₁₀. Various studies have consolidated PBL stature in numerous regression examinations (Liu et al. 2007; Green et al. 2009; Glantz et al. 2009; Di Nicolantonio et al. 2009; Schapp et al. 2009; Wang et al. 2010; Tsai et al. 2011).

One of the first to incorporate meteorology in a different regression investigation of particulate matter was led by Gupta et al. (2006). One year of AOD recoveries from MODIS on board the Terra and Aqua satellites alongside ground estimations of PM₁₀ were utilized to survey air quality more than 26 areas in and around Sydney, Delhi, Hong Kong, New York City, and Switzerland. A relationship coefficient of 0.96 was gotten between bin averaged value of day by day mean AOD and ground-level PM₁₀ when boundary layer height and wind pace were joined in the model. The best results were gotten when boundary layer heights were less created (100-200m) and with fewer than 25% overcast spread.

Tian and Chen (2009) utilized numerous regression investigations to anticipate hourly concentrations of PM₁₀ on a territorial premise for southern Ontario, Canada. They looked to further improve the effectively settled relationship amongst AOD and PM₁₀ concentrations on the ground by including boundary layer and meteorological parameters. The objective of this study was to give a financially savvy way to deal with supplementing ground-based observing stations. Information from 2004 was utilized to create and approve the model and the model-anticipated qualities were profoundly corresponded with ground-based perceptions with a R² of 0.64.

Wang et al. (2010) examined whether including relative humidity from meteorological stations and LIDAR determined boundary-layer height would enhance the AOD-PM₁₀ relationship in Beijing, China over a 15-month era (July, 2007 through October, 2008). Including the boundary layer stature and relative humidity enhanced the model by 14% (R₂ = 0.48 for 2-variable study; R₂ = 0.62 for multivariate study).

Lee et al. (2011) proposed a technique to align MODIS AOD information to precisely anticipate ground-level PM₁₀ concentrations. They guarantee it is the primary study to build up PM₁₀- AOD relationship regularly. MODIS installed on the Terra and Aqua satellites was utilized to recover AOD information. The study territory secured parts of Massachusetts and Rhode Island and was partitioned into 387x10 km² networks utilizing QGIS rendition 9.3. Measured and anticipated yearly mean PM₁₀ concentrations were factually looked at utilizing numerous regression connection coefficients. Lee et al. gotten a higher relationship (R = 0.79, R² = 0.62) utilizing the numerous regression model when contrasted and a straightforward direct regression of the same information (R² = 0.26; R = 0.5) and infer that the execution of the multivariate model to anticipate surface-level PM₁₀ concentrations is better than a basic two

variable straight regression model and that this strategy would be appropriate for both time-arrangement and cross-sectional health impact thinks about.

Mao et al. (2011) developed and tested an enhanced land-use regression (LUR) model that incorporated monthly AOD data from MODIS Terra. Typically, LUR models use variables such as land use/land cover, point-source emission estimates, population, and traffic-information to predict the long-term intra-urban distribution of air pollutants. A problem with this method is that it lacks temporal variability and is often limited in representing the spatial variability of pollutants. The predicted concentrations were higher during summer/fall and are consistent with previous studies from the eastern United States (Chu et al. 2003; Zhang et al. 2006). This is likely due to the high humidity, temperatures and strong insolation that cause atmospheric ions to react and form aerosol products.

A study was led by Tsai et al. (2011) explored utilizing three years (2006-2008) of surface particulate matter and MODIS AOD recoveries to evaluate the capability of satellite based air quality observing in Taiwan. Relative humidity and boundary layer statures were consolidated as autonomous variables. Two sun photometers were utilized to approve the MODIS AOD recoveries ($R^2 = 0.82$ for Terra; $R^2 = 0.69$ for Aqua). The stature of the boundary layer was observed to be basic to the AOD- PM_{10} relationship as clear from the higher connections ($R^2 = 0.77$ to 0.86) found in the fall and winter when a steady and very much blended boundary layer prevails. Relationship did not surpass 0.67 amid the spring and summer when monsoonal streams cause solid convective blending and instability.

Some of the studies over Indian Subcontinent have used various dataset and different statistical parameters for analysis of AOD Data.

A similar study was directed by Mansha and Ghauri (2011) for the seasonal and spatial variety of aerosol concentrations over Karachi, Pakistan utilizing MODIS AOD from the Terra and Aqua satellites, sun photometers, and ground-based PM_{10} and meteorological estimations from 2008. Higher PM_{10} concentrations were recorded in the winter over summer, potentially because of lower boundary layer statures amid winter and expanded wind speed amid the late spring rainstorm months. MODIS AOD, temperature, relative moistness, and wind speed variables anticipated PM_{10} estimations with a R^2 somewhere around 0.47 and 0.67 when compared and the everyday recorded mean, with the most noteworthy correlations amid winter.

A K Prasad et. al.(2004) learns about variability of aerosols in Indian subcontinent. Indo-Asian aerosols have sway on radiative compelling that cause negative driving (cooling) at surface and positive outcome (warming) at top of atmosphere (Satheesh and Ramanathan, 2000; Ramanathan et al. 2001b; Kaufman et al., 2002). Ramanathan et al. (2001a) have observed that this extra warming and cooling influence tropical precipitation designs and disturbs hydrological cycle. AOD dispersion amid pre-storm influences the cloud arrangement and consequently precipitation conveyance. AOD is observed to be high ($>.6$) in Ganga bowl with expanding aerosol fixation at a disturbing rate in eastern piece of bowl in most recent four years (Fig. 1, summer 2000 and 2004). Southern parts of India demonstrate a much cleaner environment with AOD under 0.4. The spatial slope of AOD is indicating increment from southern piece of Indian subcontinent to northern part up to Himalaya. The focal India indicates moderate AOD values. The Gujarat state in western India likewise demonstrates a high AOD in summer because of impact of Thar Desert in its north-east area furthermore transport of dust from Middle East (Dey et al. 2004). Contribution of aerosols (for the most part coarser division) from Thar Desert and dry season amid pre-rainstorm cause high AOD in the Ganga bowl. Fine soil dust from dry un-vegetated rural area amid summer is another huge wellspring of aerosols in this district.

Parul Srivastava et. al.(2014) Multi-sensor aerosol information sets are examined to look at the aerosol qualities over the Delhi national capital region. Both the Multiple-angle Imaging Spectroradiometer(MISR) and Moderate Resolution Imaging Spectroradiometer (MODIS) catch the occasional cycle of aerosol optical depth (AOD) as saw by ground-based estimations. Be that as it may, AOD from MISR demonstrates a low accuracy with respect to AOD from MODIS, which increments straightly at high AOD conditions. An extensive distinction (by $>25 \text{ W m}^{-2}$ per unit AOD) in the highest point of-atmosphere direct radiative forcing productivity got from MODIS and MISR-recovered AOD is seen amid the winter and pre-rainstorm seasons with respect to alternate seasons. The pervasive nearness of dust (as showed by non-circular particle portion to AOD and straight depolarization proportion qualities) is watched consistently. The aerosol layer is generally restricted to 2 km of surface in the winter and post-rainstorm seasons, while it grows past 6 km in the pre-storm and rainstorm seasons. Columnar AOD is observed to be exceptionally touchy to aerosol vertical dissemination. Aerosol vertical structure over Delhi NCR demonstrates a solid regular variety with aerosols for the most part bound underneath 2 km amid the post-rainstorm to winter seasons. In the other two seasons, the aerosol layer grows past

6 km. These vertical structures might be useful in assessing atmosphere model reproductions (e.g. Das et al. 2013).

Amit Misra et al. studied the MODIS inferred aerosol optical profundities (AODs) and correlation against the ground based perceptions from Microtops sunphotometer over Ahmedabad (72° 5_E, 23° 03_N) in Western India. The locale is semiarid and postures challenge for the satellite remote sensing of aerosols. Other than contrasting the ground truth and the Collection Version 4 of MODIS aerosol item, the paper reports the primary ever acceptance of the overhauled Collection Version 5 of the MODIS aerosol item over India. The AOD information from Aqua stage is found the middle value of more than 0.5_ _ 0.5_centered at Ahmedabad and contrasted and the sunphotometer perception taken inside thirty minutes to the satellite bridge time. The Version 4 information examination demonstrated an extensive dissipate. Further, the correlation for 470 nm and 660 nm carry on contrastingly over various years. In general, the examination indicates significant change in the Collection Version 5 aerosol item. Among seasons, Pre-Monsoon (April to May) has the best relationship and Dry season (December to March) the slightest. The overhauled item has scope for further change as the relationships are not as much as solidarity, and the degree of underestimation for 470 nm is all the more amid Dry and Post-Monsoon seasons though that for 660 nm is additionally amid Pre-Monsoon and Monsoon seasons which are commanded by fine and coarse particles separately. The outcomes demonstrate a superior surface reflectance parameterization by the MODIS Collection Version 5 calculation when contrasted with Version 4 however the aerosol model utilized as a part of the recovery calculation is still not satisfactory.

With regards to contemplating the aerosol properties and their variety along the Indo-Gangetic bowl, Jethva et al. (2005) looked at the month to month mean AOD at 550 nm registered from MODIS Level 3 every day gridded information with the AERONET sunphotometer determined month to month mean AOD values from Kanpur, India for the period January 2001 to July 2003. They found a precise overestimation by MODIS amid summer and an underestimation amid winter (Jethva et al., 2005).

The redesigned MODIS aerosol item with better surface reflectance parameterization, upgraded aerosol models and different adjustments to the recovery strategy, demonstrates a gigantic change in every one of the parameters of the relationship plot. The captures for all years and all seasons are under 0.05 at both 470 and 660 nm. Among every one of the years, 2005

demonstrates the best relationship with R^2 Blue = 0.71 and R^2 Red = 0.75. SlopeBlue = 0.78 and SlopeRed = 0.90 are nearest to solidarity and captures are most minimal during the current year when contrasted with different years-a component identified with the most astounding precipitation got amid this year when contrasted with others which lessens the surface reflectance. Pre-Monsoon season demonstrates the best connection among every one of the seasons with R^2 Blue = 0.73, R^2 Red = 0.81, SlopeBlue = 0.84, SlopeRed = 0.81, InterceptBlue = 0.01 and InterceptRed = -0.0005 . Further, this season demonstrates the most extreme change in relationship from the C004 information which is ascribed to the better parameterization of surface reflectance in the redesigned item which is typically high amid this season.

2.4 Summary of literature review:

A survey of the late writing indicates local and seasonal varieties in the relationship amongst AOD and PM_{10} with generally shifting results. Better results were found in the eastern United States in the spring and summer, which is likewise when fine particulate concentrations are most noteworthy (Engle-Cox 2003; Zhang et al. 2006; Mao et al. 2011). On the other hand, thinks about situated in south Asia and north focal Italy had the most astounding concentrations and relationships amongst's AOD and PM_{10} amid the fall and winter (DiNicolantonio et al. 2009; Mansha and Ghauri 2011; Tsai et al. 2011). The writing likewise demonstrates that the consideration of meteorological parameters, for example, PBL, temperature, and relative humidity, enhanced model results over those that lone consolidated AOD and PM_{10} in the regression models.

Likewise, these particles disperse and retain light. As their levels in the atmosphere build, they can cut the sum daylight that achieves the ground furthermore influence the degree to which heat from the planet escapes into space. Aerosols in this manner have an impact on the atmosphere. Aerosols incorporate actually happening particles like sea salt and tidy. Yet, concern has becoming over those created by people, for example, residue from vehicle discharges and the copying of kindling and sulfate particles that heave out from warm power stations and cement plants.

A number of the stations in India had aerosol information over just the previous decade or somewhere in the vicinity. In any case, the Thiruvananthapuram and Visakhapatnam stations had information that did a reversal about 30 years. Over a large portion of the stations, AOD had demonstrated an expanding pattern. This demonstrated the AOD "over the landmass is not just expanding relentlessly, even the rate of expansion has additionally expanded, the circumstance being all the more disturbing over the industrialized eastern waterfront area (Visakhapatnam)," watched S. Suresh Babu and alternate researchers in a paper distributed in the examination of the AOD levels at four distinct wavelengths of light made it conceivable to observe fine human-created aerosols from the coarse ones that were normally delivered. The relative wealth of aerosols created by people had developed at both Thiruvananthapuram and Visakhapatnam, the ascent being more noteworthy at the last mentioned.

Climate models utilized by researchers to study what could happen in the coming decades were not checking this colossal development in aerosol levels. In the event that the present pattern in India of expanding anthropogenic aerosol emanations were to proceed unabated, the stacking of such particles in the atmosphere could increment at more prominent rate. The aerosol-prompted warming of the atmosphere may triple subsequently, which could influence the rainstorm and the territorial atmosphere (Satheesh et. al.2012),Intergovernmental Panel on Climate Change.

Chapter 3

Methodology

3.1 General

This chapter outlines the steps taken in this research and the research questions, designs, adopted methods, sample selection, data collection and analysis. The mapping of AOD is useful in understanding the functional relationships between atmospheric models and ground monitoring systems. These factors among the backscatter, radiance, clouds condition, and atmospheric refraction are useful in understanding and modelling the causation, spatial distribution of Aerosols. Furthermore AOD mapping and research allows us to predict the levels of PM₁₀ in the atmosphere and enhance their prevention and intervention strategies.

3.2 Study Area

Shimla is situated in the Central Himalayas at 31° 4' to 31° 10' north latitude and 77° 5' to 77° 15' east longitude.. The topography of Shimla is characterized by rugged mountains, steep slopes and deep valleys. Shimla is located at an altitude of 2206 meters above mean sea level. It experiences cold winters during December – February, with temperatures ranging from -4°C to 13°C. .

3.2.1 Topography

The topography of Shimla is characterized by rugged mountains, steep slopes and deep valleys. It has an average altitude of 2,206 meters (7,238 ft) above mean sea level and extends along a ridge with seven spurs. Shimla lies in the south-western ranges of the Himalayas at 31.61°N 77.10°E. It has an average altitude of 2,206 meters (7,238 ft) above mean sea level and extends along a ridge with seven spurs. The city stretches nearly 9.2 kilometers (5.7 mi) from east to west.

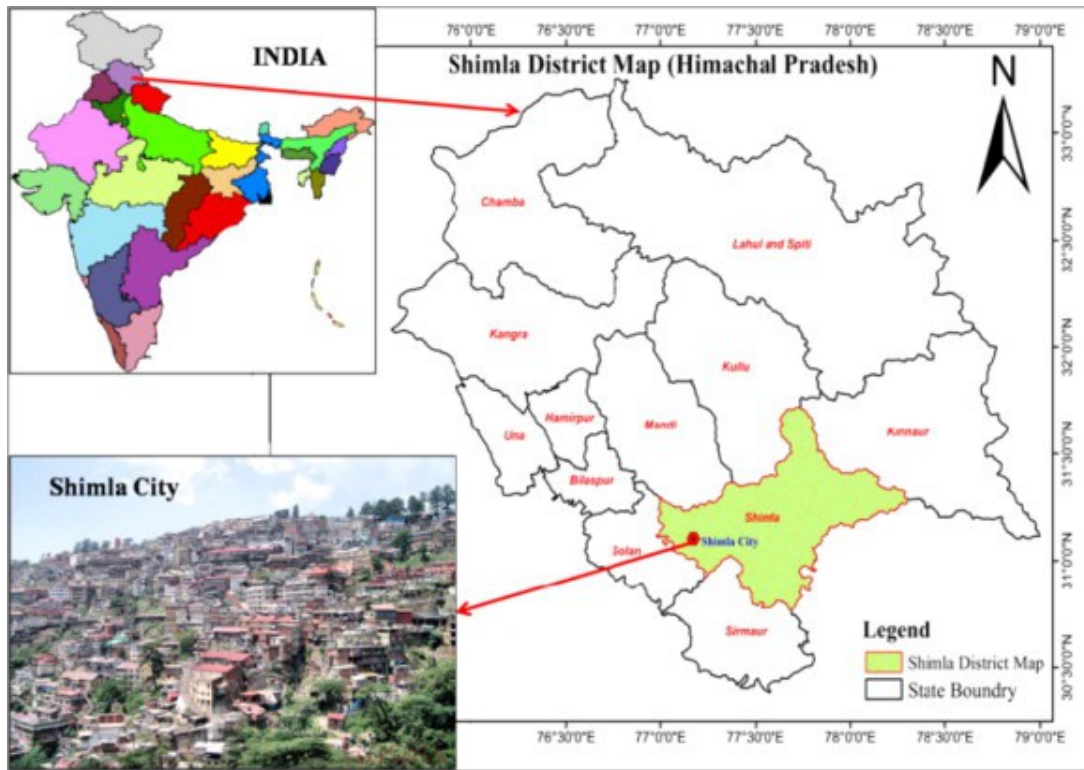


Figure 12 Geographical Location of Shimla City

3.2.2 Climate

The winter temperature in Shimla varies from 18°C to -4°C and in summer from 26°C to 10°C. The city receives the monsoon during the months of July to September with annual average rainfall of about 150 mm.

The summers (May – June) are mild with temperatures varying from 20°- 30°C. The monsoon period extends from June to September and records moderate rainfall. The average rainfall recorded for the last 25 years (1980 – 2005) in Shimla is 1437 mm. As per Census (2011), Shimla is the only Class I City in the State of Himachal Pradesh with total population of 169,758 persons

3.3 MODIS

MODIS (or Moderate Resolution Imaging Spectroradiometer) is a key instrument aboard the Terra (originally known as EOS AM-1) and Aqua (originally known as EOS PM-1) satellites. Terra's orbit around the Earth is timed so that it passes from north to south across the equator in the morning, while Aqua passes south to north over the equator in the afternoon. Terra MODIS

and Aqua MODIS are viewing the entire Earth's surface every 1 to 2 days, acquiring data in 36 spectral bands, or groups of wavelengths (see MODIS Technical Specifications). These data will improve our understanding of global dynamics and processes occurring on the land, in the seas, and in the lower atmosphere. MODIS is playing a vital role in the development of validated, global, interactive Earth system models able to predict global change accurately enough to assist policy makers in making sound decisions concerning the protection of our environment.

MODIS (or Moderate Resolution Imaging Spectroradiometer) is a key instrument on board the Terra (known as EOS AM-1) and Aqua (known as EOS PM-1) satellites. Terra's orbit around the Earth is planned with the goal that it goes from north to south over the equator in the morning, while Aqua ignores south to north the equator toward the evening. Terra MODIS and Aqua MODIS review the whole Earth's surface each 1 to 2 days, obtaining information in 36 spectral bands, or gatherings of wavelengths. This information will enhance our comprehension of worldwide progression and procedures happening on the area, in the seas, and in the lower atmosphere. MODIS is assuming an essential part in the advancement of approved, worldwide, intelligent Earth framework models ready to anticipate worldwide change precisely enough to help arrangement creators in settling on trustworthy choices concerning the security of our surroundings.

3.3.1 Orbit and Acquisition Characteristics

The Terra satellite began collecting data of the Earth's surface in February of 2000. It is a polar orbiting spacecraft that obtains complete Earth coverage every one to two days and is designed to cross the equator at a time when cloud cover is at its daily minimum (10:30AM, descending). The following table describes the orbit and acquisition characteristics of the MODIS sensor onboard the Terra satellite.

Swath (km)	Scene Size (km)	Altitude (km)	Revisit (days)
2330km	~10 x ~10	705km	16

3.3.2 Radiometric Characteristics

Unlike other satellite imagery and items, MODIS information is deliberately changed over into determined atmospheric, oceanic, and terrestrial items. The MODIS surface reflectance product is a piece of the last mentioned. Each of the seven area bands are rectified for atmospheric impacts with a calculation that utilize aerosol and water vapor data gathered by the sensor. The calculation redresses for slender cirrus clouds, aerosols, and atmospheric gasses. The outcome is an estimation of surface reflectance as though it had been measured at first glance, without the impacts of atmospheric retention or dispersing. The table 6 underneath depicts wavelengths spoke to by the 5 bands incorporated here:

Table 6 Wavelength and spectral resolution for study of aerosols

Band	Wavelength (nm)	Description	Resolution (m)	Primary Use
1	620–670	Red	250	Land/Cloud/Aerosols Boundaries
2	841–876	Near-infrared	250	
3	459–479	Blue	500	Land/Cloud/Aerosols Properties
4	545–565	Green	500	
5	1230–1250	Short wave infrared	500	

3.3.3 MODIS Aerosol Product

The MODIS Aerosol Product screens the encompassing aerosol optical thickness over the seas internationally and over a segment of the landmasses. Further, the aerosol size dissemination is determined over the seas, and the aerosol sort is inferred over the mainlands. Every day Level 2 information are created at the spatial determination of a 5x5 1-km (at nadir)-pixel exhibit. There are two MODIS Aerosol information item documents: MOD04_L2, containing information gathered from the Terra platform; and MYD04_L2, containing information gathered from the Aqua platform.

3.3.3 Research and Application

Aerosols are one of the sources of vulnerability in atmosphere modeling. Aerosols shift in time in space and can prompt varieties in cloud microphysics, which could affect cloud radiative properties and atmosphere. The MODIS aerosol item is utilized to study aerosol climatology, sources and sinks of particular aerosol sorts (e.g., sulfates and biomass-blasting aerosol), cooperation of aerosols with mists, and atmospheric adjustments of remotely detected surface reflectance over the area.

3.4 Data Ordering Tools & Resources

Listed below are a variety of tools and resources that can be utilized with MODIS Data. Each listing provides a link to the tool or resource and a short summary of its use.

3.4.1 Earth Data

Earth Data is a site containing an endless measure of data on use and access of all NASA Earth Observing System Data and Information System (EOSDIS) information items. All MODIS information items can be gotten to from the site. The Earth Data site gives numerous client assets, including instructional exercises, online courses, and also data hunt, disclosure and handling data. Discipline particular data (e.g. Atmosphere, Cryosphere, Land, Sea, Human Dimensions) is likewise included on the site. The device is utilized of recognizing the datasets to be utilized for the study and preparing of the data.

<http://earthdata.nasa.gov/>

3.4.2 Giovanni

Giovanni and Giovanni 4 are Web applications created by the GES Disk to give a straightforward, natural approach to imagine, break down, and get to Earth science remote sensing information, including large information volumes, especially from satellites, without downloading the information. The MODIS Atmosphere information items are accessible to dissect with this apparatus. The apparatus is utilized to envision the information online to have a general thought of the aerosols dissemination over North India.

<http://disc.sci.gsfc.nasa.gov/giovanni/overview>

<http://giovanni.gsfc.nasa.gov/giovanni/>

3.4.3 HDF-EOS to GeoTIFF converter (HEG)

The HDF-EOS to GeoTIFF converter (HEG) instrument changes over MODIS hdf arranged information records into GeoTIFF, local double or HDF-EOS Grid. The HEG device additionally has reprojection, resampling, subsetting, mosaicing and metadata creation capacities. This apparatus is utilized to change over information from HDF configuration to GeoTIFF group which is less demanding to work with on a GIS platform.

<http://hdfeos.org/software/heg.php>

3.4.4 HDF Explorer & HDF Look

The above two instruments are information perception programs that read HDF documents and permits the client to envision these records. Both devices are applicable to all MODIS information items in HDF group. This instrument is utilized of recognizing the information sets and the AOD values connected with the geolocations of the checking stations..

<http://www.space-research.org/>

<http://www-loa.univ-lille1.fr/informatique/index.php?/>

3.4.5 LP DAAC2Disk Download Manager

The LP DAAC2Disk Download Manager allows users to simplify the search and http download process using the LP DAAC's data pool holdings. Users have the option of using a web-based interface or script to retrieve their data. The web-based interface is available from the [LP DAAC Data Pool web page](#). The LP DAAC2Disk utility is also available as a script that can be downloaded and executed from the command line (available in Windows, Linux/Unix and Machintosh platforms). The script and user guide scripting options are available from the [LP DAAC Data Pool web page](#).

https://lpdaac.usgs.gov/data_access/data_pool

3.4.6 MODIS Level 1 Atmosphere Archive and Distribution System (LAADS Web)

LAADS Web is the web interface to the Level 1, Atmosphere Archive and Distribution System. LAADS Web provides quick and easy access to all MODIS Level 1, 2 and 3

Atmosphere and Land data products with a number of post processing options. Post processing options include subset by parameter, area or band, mosaiced, reprojected or masked. The website also provides quick look true color RGB and false color images of selected data sets. This tool is used to download the data from MODIS archives.

<https://ladsweb.nascom.nasa.gov>

3.4.7 MODIS Swath Reprojection Tool (MRT Swath) and MODIS Reprojection Tool (MRT)

The MODIS Swath Reprojection Tool reads MODIS swath HDF-EOS files and produces binary HDF-EOS Grid or GeoTiff files of gridded data in different map projections. The MODIS Reprojection Tool reprojects MODIS Level-2G, Level 3 and Level 4 land data products to a user specified output map projection type and output resolution. The MODIS Reprojection Tool is developed and maintained by the LP-DAAC and is available for free to all registered user. This tool is used for aligning the images with the geolocations and for trimming the image.

https://lpdaac.usgs.gov/tools/modis_reprojection_tool_swath

https://lpdaac.usgs.gov/tools/modis_reprojection_tool

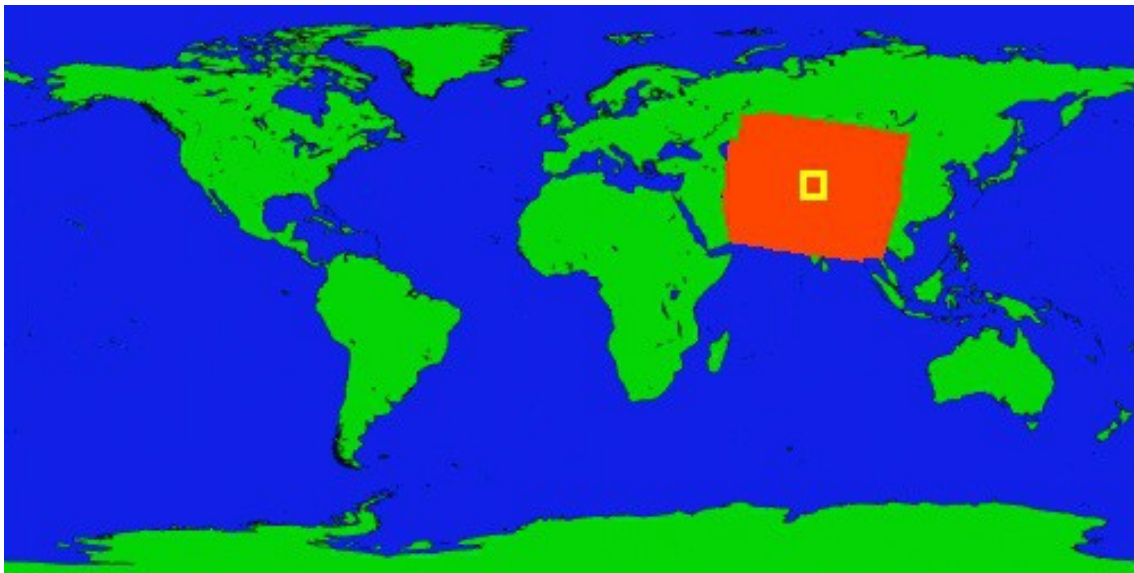


Figure 13 Study Area Selected

3.5 MISR

The Multi-angle Imaging Spectro Radiometer (MISR) is an investigative instrument on the Terra satellite dispatched by NASA on December 18, 1999. This gadget is intended to quantify the solar radiation reflected by the Earth framework (planetary surface and atmosphere) in different bearings and spectral bands; it got to be operational in February 2000. Information produced by this sensor have been demonstrated valuable in an assortment of utilizations including atmospheric sciences, climatology and checking terrestrial procedures.

The MISR instrument comprises of a creative setup of nine separate advanced cameras that assemble information in four diverse spectral bands of the sunlight based range. One camera indicates the nadir, while the others give forward and toward the back ward view points at 26.1° , 45.6° , 60.0° , and 70.5° . As the instrument flies overhead, every area of the Earth's surface is progressively imaged by every one of the nine cameras in each of four wavelengths (blue, green, red, and near infrared).

The information assembled by MISR are helpful in climatological studies concerning the mien of the sunlight based radiation flux in the Earth's framework. MISR is particularly intended to screen the month to month, seasonal, and long term patterns of atmospheric aerosol particle concentrations including those framed by common sources and by human exercises, upper air winds and overcast spread, sort, stature, and in addition the portrayal of land surface properties, including the structure of vegetation shelters, the appropriation of area spread sorts, or the properties of snow and ice fields, amongst numerous other biogeophysical variables.

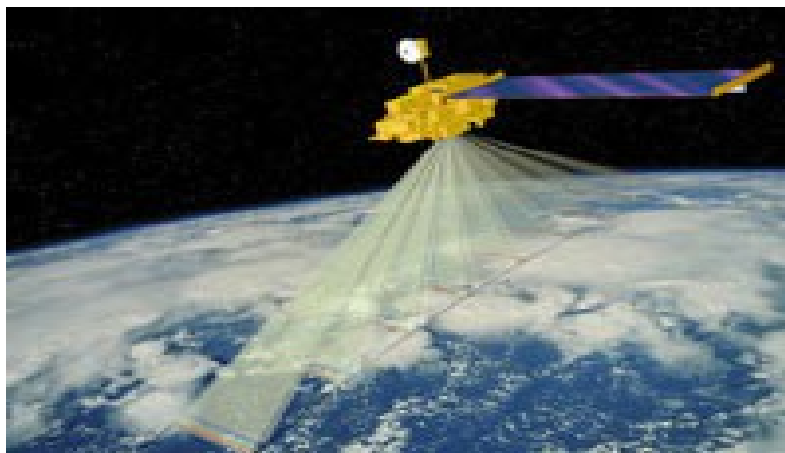


Figure 14 Satellite remote sensing

3.6 Ground Sensors Data

PM₁₀ ground observations are measured by the Himachal Pradesh Pollution Control Board under the national ambient air quality program which was started in 1986-87 with the objective to find the current status of pollution and to study the trends as the result of increasing industrialization. Under NAAQM a network was established in the city also to monitor the pollution there are two monitoring stations. The concentration of PM₁₀ in Shimla city is growing every year. The analysis of the data maintained by the Himachal Pradesh Pollution Control Board (HPPCB) shows a significant increase in the concentrations of PM₁₀. The data is measured at two monitoring stations out of which one is at Takka Bench, The Ridge (Station-1) and the other is at ISBT, Shimla (Station-2).



Figure 15 Monitoring station 1 at “The Ridge” (Takka bench).



Figure 16 Monitoring station-2 at “Old ISBT”.

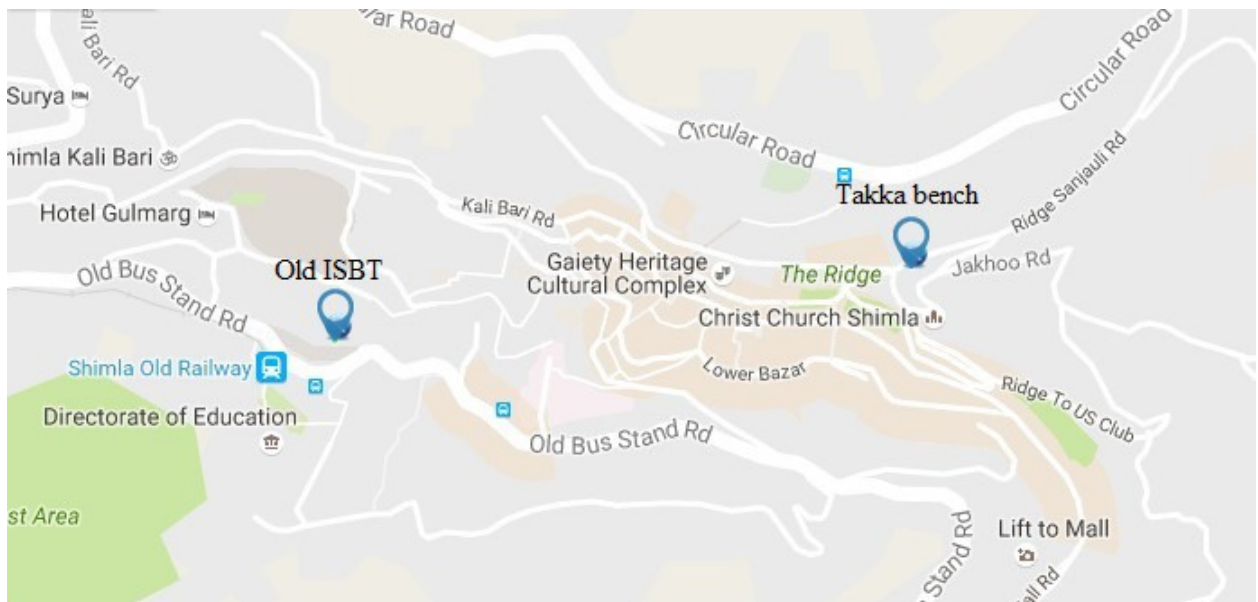


Figure 17 Location of monitoring station

3.7 Satellite Sensors Data

MODIS information were from Terra MODIS which passes over Shimla in the late morning. MOD04 Level Two Aerosol Product incorporates AOD values contained in the variable Corrected Optical Depth Land in a 10 kilometer determination. Because of value confirmation and a dry-land study range, the best information field to utilize is the Corrected Optical Depth Land (Remer et al., 2005). All MODIS information were downloaded from the NASA Laads site (Horrocks, 2008). NASA Laads site permitted inquiries of the spatial, fleeting, ghastrly qualities and change of the information to GeoTiff design. The alternative to download the first Hierarchical Data Format (HDF) records were additionally accessible. Information were downloaded from January through January 2013 to December 2015, individually. The MISR sensor is likewise on board the Terra satellite. MISR ways 64, 65, and 66 had the best scope of the whole North India; accordingly information were downloaded for all days on those ways. Level two Aerosol information MIL2ASAE, were requested from the NASA Langley ASDC MISR request and customization device, (Krusterer, 2008). MISR AOD information were separated at 558 nm utilizing the field name Reg Best Estimate SpectralOptDepth as was shown in "Liu et al. 2006." MISR documents were just accessible as HDF format only.

3.7.1 Satellite Sensor HDF Files

Hierarchical Data Format (HDF), were created to be a standard method of data storage for large amount of data collected. HDF files are easy to share and can be used with an assortment of software and programming languages. HDF format is the official data format for the NASA Earth Observing System, which includes MODIS and MISR products.

3.7.2 GeoTIFF Files

GeoTIFF documents are turning out to be progressively prominent in remote sensing. They permit more clients access to remotely detected information including satellite symbolism. GeoTIFF documents are basically TIFF pictures with geographic metadata installed in one or more structures, including yet not restricted to, projection, georeferencing, and can be utilized as a part of any GIS, CAD or picture preparing programming (Ruth, 2005). In the event that all the NASA satellite items could be effortlessly changed over into GeoTIFF format then the information would be considerably more open to the overall population and specialists.

3.7.3 Satellite Sensors Data Processing

The essential satellite AOD information source was the MODIS sensor. MODIS was chosen for its higher worldly determination, recurrence, and more extensive swath width covering a larger part of the city. MODIS gave more information to correspond with ground observing and satellite inferred AOD. For fast data preparing, GeoTIFF pictures were procured of the MODIS information specifically from the previously stated site. Utilizing the picture post preparing choices the GeoTIFF records were requested. These pictures had the appropriate AOD information is much simpler to oversee than HDF . Utilizing QGIS all the AOD values from the GeoTIFF pictures were separated. Initial a QGIS venture was made that contained a state boundary layer of Shimla and all the more essentially the areas of the all the ground sensors.

MISR information included an extra stride in handling; the HDF record was initially changed over into a GeoTIFF utilizing the HDF EOS to GeoTIFF (HEG) converter. The HEG instrument permitted HDF documents to be changed over and anticipated for use in business programming that can't read HDF records. Handling time expanded, however the quantity of MISR records were impressively less than MODIS. Since MODIS documents were changed over to GeoTIFF format before download, MISR HDF records were changed over to GeoTIFF documents to keep up record formats among the satellite information.

3.7.4 Satellite Sensors Data Extraction

For the MODIS and MISR AOD values, information was extracted for the nine sites at eight ground monitoring locations in three ways using the pixel inspector in GrassGIS. First for MODIS, all values in a 5 x 5 pixel square around each site were extracted, and then the median values for the 5 x 5, 3 x 3 and the centroid pixel were calculated. The median values allowed for an easier spatial comparison between data. The same locations were extracted from MISR data using the 3 x 3 method, finally calculating 3 x 3 median and the centroid. Extracting a 5 x 5 median filter of pixel values for the MODIS 10 km data and a 3 x 3 median filter for the MISR 17.6 km data makes the two resolutions relatively comparable (Liu et al., 2006). Median filters allowed for increased accuracy and created acceptable values if some of the measured pixels had

no data (Chu, et al. 2002). If the date of the data did not have fifty percent of the pixels present in the median filters the date was eliminated from the statistical analysis.

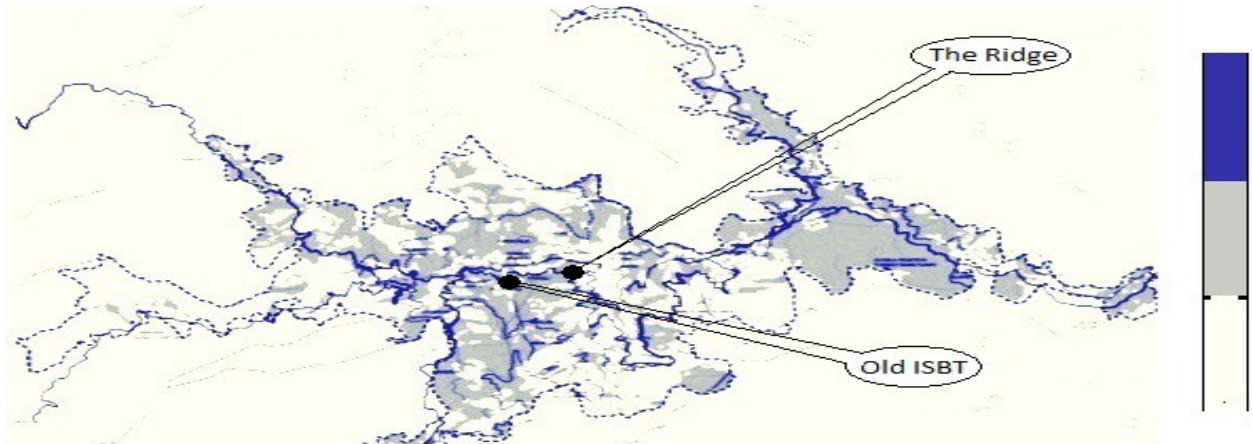


Figure 18 MODIS AOD over Shimla city for January 2011.

Chapter 4

Data Analysis and Results

The concentration of PM₁₀ in Shimla city is growing every year. The analysis of the data maintained by the Himachal Pradesh Pollution Control Board (HPPCB) shows a significant increase in the concentrations of PM₁₀. The data is measured at two monitoring stations out of which one is at Takka Bench, The Ridge (Station-1) and the other is at ISBT, Shimla (Station-2).

4.1 Station-1 (Takka Bench) The Ridge

This station is at elevation of 2210m above mean sea level and falls under 'C' category of sensitive area zone.

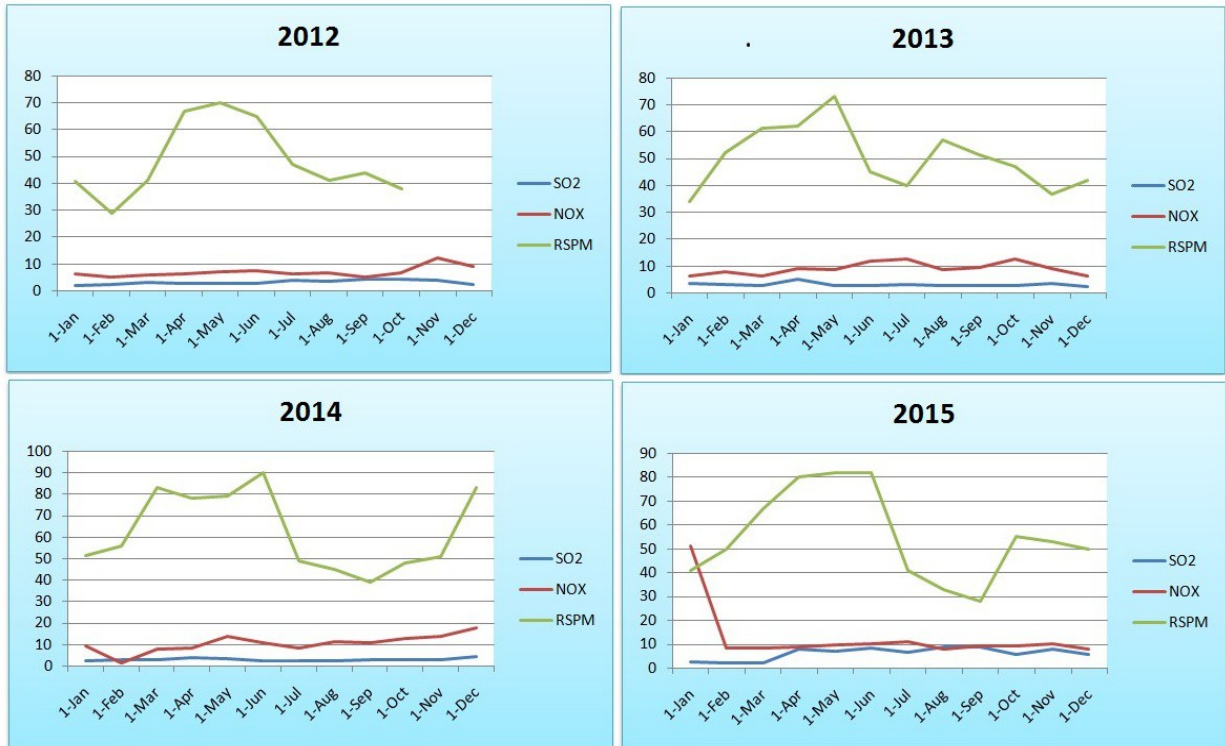


Figure 19 Variation of PM₁₀ at station 1 during 2012 - 2015

4.2 Station 2 (Old ISBT Shimla)

The station is located on the top of ISBT in midst of commercial and residential zone at a comparatively lower height of about 2050m from mean see level. It falls under residential area zone 'B' category.

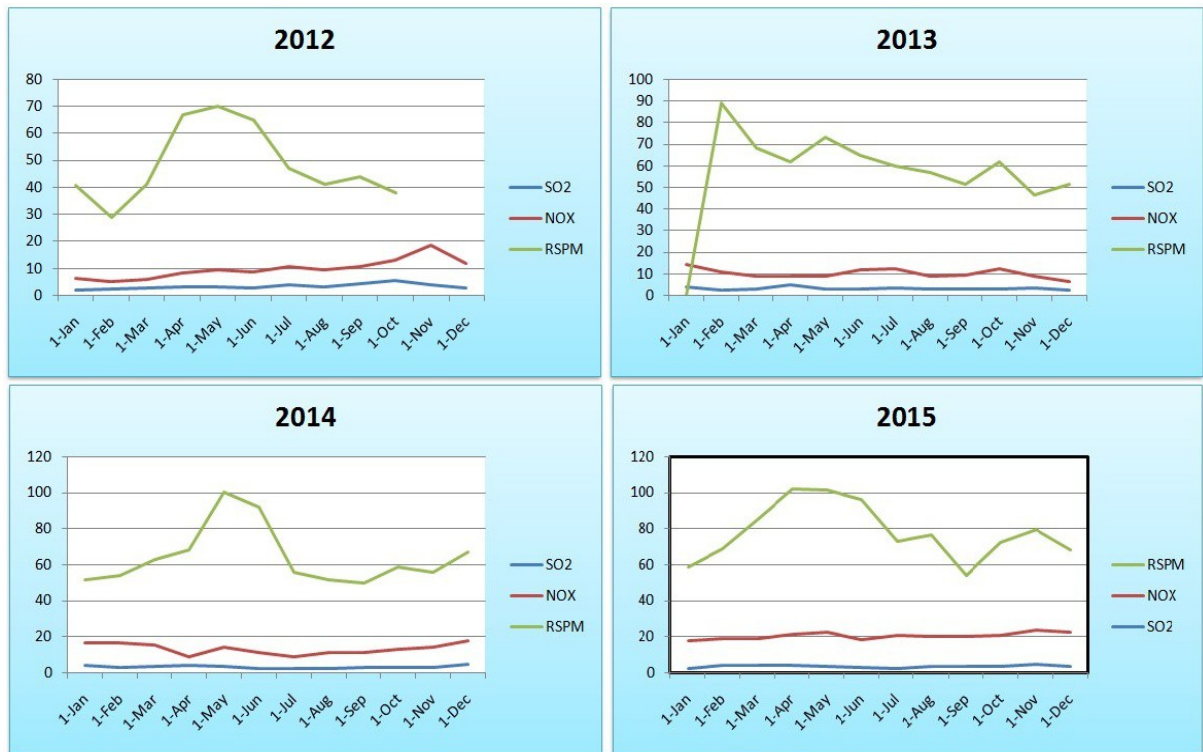


Figure 20 Variation of PM₁₀ at station 2 during 2012 - 2015

The data clearly indicate not only the increase in the concentration of Particulate Matters but also the rate of increase in the concentration is also increasing. There has been a drastic change in the Temperature of the city. During winter season the minimum temperature of Shimla is warmer by approximately 7°C.

4.3 Data availability and Coincidence

A huge issue with satellite information is the absence of consistency in accessibility. At the point when researching aerosols, overcast days were no quality days. This is a huge hindrance for controllers to utilize satellite information to help with determining air quality. In Table 7 and Table 8, the quantity of days of information downloaded contrasted with the days with qualities for the MODIS and MISR satellite sensors changed enormously. The ground sensors were uninhibited by the shady climate and kept on gathering information. Another huge issue was while associating the information sorts the days got to be restricted by accumulation date. The PM ground sensors just gathered information at regular intervals and the satellite sensors are

restricted to atmospheric conditions; this brought about just 458 days of PM sensors agreeing with MODIS and just 212 days harmonizing with MISR. This essentially eliminated MISR from any sort of practicality as a regular measurement monitor.

Table 7 Days of data available from collected data sources at The Ridge.

Data source	2013	2014	2015
MODIS	80	81	74
MISR	42	39	32

Table 8 Days of data available from collected data sources at bus stand.

Data source	2013	2014	2015
MODIS	79	73	71
MISR	33	35	31

Due to availability of only one data set to measure particulate matter, the spatial area that was investigated is limited. Within two standard deviations of the mean values the regression in Fig 21. shows a very good relationship between HPPCB PM₁₀ data and MODIS data.

Figure 21 Regression of MODIS AOD and Ground PM₁₀ (over all) n=458

In Shimla, of the 458 coincident days between the datasets, just 2 days from the MISR dataset and 7 days from the MODIS dataset surpassed the NAAQS 24 hour standard of 35ug/m³ for PM₁₀. The rest of the MISR destinations had no days that surpassed the NAAQS standards, however the MODIS sites did, Days that the PM₁₀ surpassed NAAQS gauges there were connections between PM₁₀ and satellite AOD.

Similarly as with the PM ground sensors, to first demonstrate a connection between's AOD sensors preceding taking a gander at the relationship between's the PM₁₀ and AOD sensors was imperative. Temporal lacks were further exacerbated by the evacuation of anomalies outside two

standard deviations demonstrates good relationship amongst MODIS and HPPCB. Information were just from the days that both MISR and MISR had values; a sum of 458 days for three year information 2012-2014. Along these lines MISR information can be utilized where MODIS information is inaccessible.

After the result of MODIS and MISR data, it was important to verify with MISR. A total of 48 coincident days of data proved beneficial to the three datasets with much higher R squared values. Table 9 shows regression values between MODIS, MISR and HPPCB data within two standard deviations of the mean. HPPCB data has an outstanding correlation with both MODIS and MISR. The MODIS 5x5 median pixel filter and the MISR 3x3 median pixel filter improved the correlation significantly with one another compared to their centroid values.

Figure 22 Regression of MODIS AOD and MISR AOD (n=186)

MODIS also had a much higher correlation with HPPCB using its 5x5 median pixel filter versus the 3x3 or centroid values. The examples below show the linear regressions between MODIS 5x5 median AOD with NAAQS AOD, MODIS 5x5 median AOD with NAAQS AOD and MISR 3x3 median AOD with NAAQS AOD respectively.

Table 9 R² values for AOD sensors, MODIS, MISR and NAMP

MODIS - MISR –NAMP			
R Squared values	MISR 3x3	MISR centroid	NAMP(Ground data)
MODIS 5x5	0.55	NIL	0.76
MODIS 3x3	0.42	NIL	0.88
MODIS centroid	NIL	0.85	0.74
NAAQS	0.65	0.38	NIL

The India Meteorological Department (IMD) designates four climatological seasons:

- **Winter**, occurring from December to March. The year's coldest months are December and January, when temperatures average around 10–15 °C (50–59 °F) in the northwest; temperatures rise as one proceeds towards the equator, peaking around 20–25 °C (68–77 °F) in mainland India's southeast.

- **Summer** or **pre-monsoon** season, lasting from April to June (April to July in northwestern India). In western and southern regions, the hottest month is April; for northern regions of India, May is the hottest month. Temperatures average around 32–40 °C (90–104 °F) in most of the interior.
- **Monsoon** or **rainy** season, lasting from July to September. The season is dominated by the humid southwest summer monsoon, which slowly sweeps across the country beginning in late May or early June. Monsoon rains begin to recede from North India at the beginning of October. South India typically receives more rainfall.
- **Post-monsoon** or **autumn** season, lasting from October to November. In the northwest of India, October and November are usually cloudless. Tamil Nadu receives most of its annual precipitation in the northeast monsoon season.

Figure 23 Regression of MODIS AOD and ground PM₁₀ during winters (n=88)

Figure 24- Regression of MODIS AOD and ground PM₁₀ during summer season (n=69)

Figure 25 Regression of MODIS AOD and ground PM₁₀ during monsoon season (n=42)

Figure 26 Regression of MODIS AOD and ground PM₁₀ during autumn season (n=53)

Figure 27 Regression of MODIS AOD and ground PM₁₀ overall. (n=458)

4.4 AOD Sensors and PM₁₀ Sensors

Due to the lack of data for MISR, it was eliminated from the data processing with the PM₁₀ data. This left HPPCB data only to correlate in Shimla and MODIS data to compare with all the sites. There is a good correlations between MODIS AOD sensor and PM₁₀ sensor. In Shimla, HPPCB data and MODIS showed a correlation through regression. Using a logarithmic scale shows a distinct relationship that correlated daily fluctuations of air quality. There were slight improvements comparing the data when applying the 50 percent pixel presence rule. The improvements were significant enough to show a direct correlation between the two types of data.

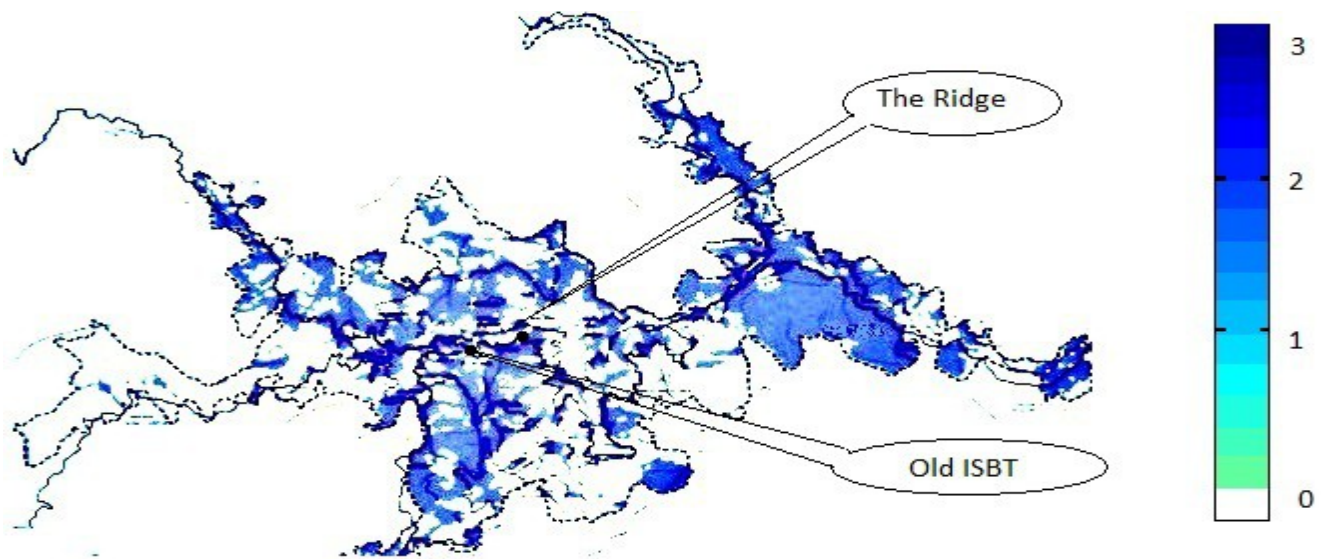


Figure 28 Aerosol distribution over Shimla in May 2013
Table 10. Summary of statistical analysis at The Ridge.

Parameters	2013	2014	2015
IA	0.97	0.88	0.99
NMSE	0.01	0.02	0.09
R	0.81	0.54	0.85
FB	0.01	0.01	0.16
F2	77	80	68

Table 11 Summary of statistical analysis at the ISBT

Parameters	2013	2014	2015
IA	0.74	0.29	0.63

NMSE	0.23	0.12	0.15
R	0.88	0.69	0.74
FB	0.03	0.17	0.16
F2	65	54	65

Table 12 Summary of statistical analysis for winter season

Parameters	2013	2014	2015
IA	0.84	0.72	0.92
NMSE	0.00	0.02	0.73
R	0.53	0.54	0.45
FB	0.01	0.01	0.16
F2	37	32	34

Table 13 Summary of statistical analysis for summer season

Parameters	2013	2014	2015
IA	0.93	0.86	0.95
NMSE	0.03	0.01	0.04
R	0.82	0.69	0.72
FB	0.01	0.08	0.04
F2	22	27	29

Table 14 Summary of statistical analysis for monsoon

Parameters	2013	2014	2015
IA	0.85	0.87	0.42
NMSE	0.07	0.05	0.14
R	0.62	0.56	0.63
FB	0.12	0.08	0.17
F2	12	17	15

Table 15 Summary of statistical analysis for autumn

Parameters	2013	2014	2015
IA	0.94	0.73	0.76
NMSE	0.09	0.12	0.00
R	0.43	0.48	0.54
FB	0.04	0.19	0.2
F2	24	19	22

Chapter 5

DISCUSSION

5.1 Data Availability

A temporal relationship between the AOD and PM₁₀ data was difficult to establish depending on the time of year. Unless there was system downtime, the ground sensors collected data regardless of the atmospheric conditions. However, the satellite data were dependent not only on orbit but also on the weather. If the weather was even partly cloudy, it was likely that the data were unusable and discarded. Pixels with missing data appear white. These white areas have no data due to cloud cover, colored pixels represent AOD values.

5.2 AOD Sensors

Similar to the PM₁₀ ground sensors, correlating the AOD sensors is important. After the initial comparison of the data days for the AOD sensors, MISR data is eliminated from the analysis as the days coinciding with the ground data were very few. MISR data can be used where MODIS Terra data is unavailable.

5.3 PM₁₀ and AOD relationship

After demonstrating that the PM₁₀ data-sets compared well with one another and select AOD datasets compared well with one another, comparing AOD and PM₁₀ was possible. The relationship was found between the AOD data and the PM₁₀ data after the removal of cloudy and rainy days. With pixel presence and the removal of outliers, the relationships were significant enough to a level worth deeming as a legitimate correlation.

Chapter 6

Conclusion

The analysis shows the air quality at station 2 is comparatively poor than station 1 or the PM₁₀ concentration at station 2 is greater than the station one. The main reason for which is more vehicular traffic in the vicinity of station 2. In fact the images show this trend throughout the year of study. There was relatively more density of particulates around roads of city.

The summer season is the time duration in which the PM₁₀ concentration is maximum in the city and is minimum during winter season. The analysis of data also shows a continuous increase in the concentration of PM₁₀ at both the stations throughout the study period(2011-2015).

The data clearly indicate not only the increase in the concentration of Particulate Matters but also the rate of increase in the concentration is also increasing. There has been a drastic change in the Temperature of the city. During winter season the minimum temperature of Shimla is warmer by approximately 7°C which is direct consequence of degraded air quality and rapid urbanization.

As direct correlations have worked elsewhere in the world to show a relationship between PM₁₀ and AOD data, the relationship was found between PM₁₀ and AOD data in Shimla varied with the seasons. The instruments of similar measurements validated one another, which holds potential in developing a better understanding of the aerosols in Himalayan region. The vetted interests in the air quality of the Shimla will no doubt help to drive the investigation of how to validate a relationship between PM₁₀ and AOD. As an enhanced tool for regulators and policy makers, there is great potential for use of satellite data to assist in determining air quality.

- The results indicated clear seasonal and annual variations.
- Major contributor to aerosol pollution is vehicular exhaust and road dust.
- The turbidity level is found to be higher for May than April month.
- Monitoring of backscatter, speciation, relative humidity, and the elevation of the planetary boundary layer would allow for new algorithms to be used with the PM₁₀ data.
- The speciation of the particulate matter may be impacting the satellite sensors' data collection.
- The amount of rain fall plays an important role in purifying the atmosphere of the stuck aerosol particles. So the more it rains the less aerosol number of particles in the atmosphere
- Ground measured parameters after conversion are comparable with the satellite derived parameters (AOD) suggesting the satellite based measurements can be used diurnally and seasonally over areas in the absence of field instruments.
- There is a need to conduct source test for diesel and gasoline combustion using vehicles representing the local vehicle fleet.

Bibliography

- Al-Saadi, J., Szykman, J., Pierce, R. B., Kittaka, C, Neil, D., Chu, D. A., et al. (2005). Improving National Air Quality Forecasts with Satellite Aerosol Observations. *Bulletin of the American Meteorological Society* Volume 86, (Issue 9), 1249- 1261.
- Anup K Prasad, Ramesh P Singh and Ashbindu Singh 2004. Variability of aerosol optical depth over indian subcontinent using MODIS data. *Journal of Indian Society for Remote Sensing*.
- Chinnam, N., S. Dey, S. N. Tripathi, and M. Sharma. 2006. "Dust Events in Kanpur, Northern India: Chemical Evidence for Source and Implications to Radiative Forcing." *Geophysical Research Letters* 33: L08803
- Christopher, S. A., and P. Gupta. 2009. Satellite Remote Sensing of Particulate Matter Air Quality: The Cloud Cover Problem. Submitted *Journal of Air and Waste Management*.
- Chu, D. A., Y. J. Kaufman, G. Zibordi, J. D. Chern, J. Mao, C. Li, and B. N. Holben. 2003. Global monitoring of air pollution over land from the Earth Observing System-Terra Moderate Resolution Imaging Spectroradiometer (MODIS). *Journal of Geophysical Research* 108: D214661.
- Chu, D.A., Y. J. Kaufman, L. A. Remer, and B . N. Holben. 1998. Remote sensing of smoke from MODIS airborne simulator during the SCAR-B experiment. *Journal of Geophysical Research* 103 (D24): 31 979-987.
- Dey, S., and L. Di Girolamo. 2011. "A Decade of Change in Aerosol Properties over the Indian Subcontinent." *Geophysical Research Letters* 38: L14811.
- Duli Chand, Robert Wood, Steven J. Ghan, Minghuai Wang, Mikhail Ovchinnikov, Philip J. Rasch, Steven Miller, Bret Schichtel, and Tom Moore (2012) "Aerosol optical depth increase in partly cloudy conditions " *journal of geophysical research*, VOL. 117, D17207, doi:10.1029/2012JD017894

- Engel-Cox, J. A., Holloman, C. H., Coutant, B. W., & Hoff, R. M. (2004). Qualitative and quantitative evaluation of MODIS satellite sensor data for regional and urban scale air quality. *Atmospheric Environment*, 38(16), 2495-2509.
- Gupta, P., and S. A. Christopher. 2008. Seven year particulate matter air quality assessment from surface and satellite measurements. *Atmospheric Chemistry and Physics* 8: 3311–3324.
- Gupta, P., S. A. Christopher, J. Wang, R. Gehrig, Y. Lee, and N. Kumar. 2006. Satellite remote sensing of particulate matter and air quality assessment over global cities. *Atmospheric Environment* 40: 5880–5892.
- Kaufman, Y. J., D. Tanré, J-F. Léon, and J. Pelon. 2003. Retrievals of profiles of fine and coarse aerosols using lidar and radiometric space measurements." *Geoscience and Remote Sensing, IEEE Transactions on* 41 (8): 1743-1754
LAAD Archives. <http://ladsweb.nascom.nasa.gov/data/>
- Liu, Y., Franklin, M., Kahn, R., & Koutrakis, P. (2006). Using aerosol optical thickness to predict ground-level PM₁₀ concentrations in the St. Louis area: A comparison between MISR and MODIS. *Remote Sensing of Environment*, 107(1-2), 33-44.
- Liu, Y., M. Franklin, R. Kahn, and P. Koutrakis. 2007. Using aerosol optical thickness to predict ground-level concentrations in the St. Louis area: A comparison between MISR and MODIS. *Remote Sensing of the Environment* 107 (2007) :33-44.
- Mansha, M., and B. Ghauri. 2011. Assessment of fine particulate matter (PM₁₀) in metropolitan Karachi through satellite and ground-based measurements. *Journal of Applied Remote Sensing* 5 (1): 053546 1-12.
- Mao, L., Y. Qiu, C. Kusano, and X. Xu. 2011. Predicting regional space–time variation of PM₁₀ with land-use regression model and MODIS data. *Environmental Science Pollution Research* : DOI 10.10.07.
- Martin, R. V. 2008. Satellite remote sensing of surface air quality. *Atmospheric Environment* 30: 1–21.
MISR. <https://www-misr.jpl.nasa.gov/getData/accessData/>
MODIS. https://lpdaac.usgs.gov/data_access/daac2disk
- National Aeronautics and Space Administration.. *MODIS product description*. http://modis-atmos.gsfc.nasa.gov/MOD04_L2/

Natunen, A., A. Arola, T. Mielonen, J. Huttunen, M. Komppula, and K. E. J. Lehtinen. 2010. A multi-year comparison of PM₁₀ and AOD for the Helsinki region. *Boreal Environment Research* 15: 544–552.

Parul Srivastava, Sagnik Dey*, P. Agarwal, and George Basil 2014. Aerosol characteristics over Delhi national capital region: a satellite view. *International Journal of Remote Sensing*, Vol. 35, No. 13, 5036–5052.

Rajiv Ganguly, Brian M. Broderick b.2010. A hybrid model for better predicting capabilities under parallel wind conditions for NO_x concentrations from highways in Ireland. *Transportation Research Part D* 15 ,513–521

Schaap, M., A. Apituley, R. M. A. Timmermans, R. B. A. Koelemeijer, and G. de Leeuw. 2009. Exploring the relation between aerosol optical depth and PM₁₀ at Cabauw, the Netherlands. *Atmospheric Chemistry and Physics* 9: 909–925.

Tsai, T., Y. Jeng, D. A. Chu, J. Chen, S. Chang. 2011. Analysis of the relationship between MODIS aerosol optical depth and particulate matter from 2006 to 2008. *Atmospheric Environment* 45: 4777-4788.

Van Donkelaar, A., R. V. Martin, M. Brauer, R. Kahn, R. Levy, C. Verduzco, and P. J. Villeneuve. Global estimates of ambient fine particulate matter concentrations from satellite-based aerosol optical depth: development and application. *Environmental health perspectives* 118 (6): 847.

Wang, J., and A. Christopher. (2003). Intercomparison between satellite-derived aerosol optical thickness and PM₁₀ mass: Implications for air quality studies. *Geophysics Research Letters*, 30: 1–4.

Wang, J., Xu, X.G., Spurr, R., Wang, Y.X., Drury, E., 2010. Improved algorithm for MODIS satellite retrievals of aerosol optical thickness over land in dusty atmosphere: Implications

for air quality monitoring in China. *Remote Sensing of Environment* 114, 2575-2583.

Wang, Z., L. Chen, J. Tao, Y. Zhang, and L. Su. 2010. Satellite-based estimation of regional particulate matter (PM) in Beijing using vertical-and-RH correcting method. *Remote Sensing of Environment* 114: 50–63.

Zhang, H., R. M. Hoff, and J. A. Engel-Cox. 2006. The relation between Moderate Resolution Imaging Spectroradiometer (MODIS) aerosol optical depth and PM₁₀ over the United States: A geographical comparison by U.S.Environmental Protection Agency regions. *Journal of Air & Waste Management Association* 59: 1358–1369.

APPENDIX

APPENDIX-A

Monthly average particulate data of shimla

2012	SO₂ in µg/m³	NO_x in µg/m³	RSPM
Jan	2.6	51	41
Feb	2.3	8.5	50
Mar	2.1	8.5	67
Apr	7.8	8.9	80
May	6.8	9.9	82
Jun	8.4	10.3	82
Jul	6.7	11.2	41
Aug	8.7	8.1	33
Sep	8.7	9.3	28
Oct	5.8	9.3	55
Nov	7.8	10.1	53
Dec	5.8	8.3	50

2013	SO₂ in µg/m³	NO_x in µg/m³	RSPM
Jan	2.5	9.5	51.4
Feb	2.9	1.7	56
Mar	2.8	7.9	83
Apr	3.9	8.7	78
May	3.7	14.1	79
Jun	2.6	11.2	90
Jul	2.5	8.6	49
Aug	2.4	11.4	45
Sep	2.7	11.2	39
Oct	3	13.1	48
Nov	3.1	14	51
Dec	4.6	18	83


2014	SO₂ in µg/m³	NO_x in µg/m³	RSPM in µg/m³
Jan	3.4	6.5	34
Feb	3.2	8	52
Mar	3	6.5	61
Apr	5	8.9	62
May	3	8.7	73
Jun	2.9	11.7	45
Jul	3.3	12.5	40
Aug	2.8	8.7	57
Sep	2.9	9.6	51.5
Oct	2.8	12.4	47
Nov	3.6	9	36.7
Dec	2.5	6.4	41.8

2015	SO₂ in µg/m³	NO_x in µg/m³	RSPM in µg/m³
Jan	2.13	6.2	40.5
Feb	2.4	5.21	28.8
Mar	3	6	41
Apr	2.9	6.5	67
May	2.7	7.2	70
Jun	2.7	7.5	65
Jul	3.7	6.2	47
Aug	3.4	6.8	41
Sep	4.2	5.4	44
Oct	4.2	6.9	38
Nov	4.02	12.1	NA
Dec	2.4	8.9	NA

APPENDIX-B

MODIS data file example

Longitude at /mod04/Geolocation Fields/ [MYD04_L2.A2013001.0840.006.2014078044830.psgsc


Table 

0, 2 = 78.67634

	2	3	4	5	6	7	
0	78.67634	78.33362	78.001884	77.68156	77.37683	77.086586	76.80
1	78.667	78.32391	77.98593	77.66785	77.36308	77.07245	76.79
2	78.66017	78.29806	77.9672	77.65163	77.34658	77.055786	76.77
3	78.637695	78.27857	77.95479	77.637825	77.33271	77.041695	76.76
4	78.62933	78.25562	77.93879	77.62011	77.31616	77.02505	76.74
5	78.60961	78.245766	77.91972	77.60721	77.30203	77.01078	76.73
6	78.5815	78.22527	77.90282	77.58685	77.28311	76.99382	76.71
7	78.56137	78.221535	77.88259	77.56009	77.266136	76.97986	76.70
8	78.555756	78.19443	77.85782	77.53485	77.24083	76.9623	76.68
9	78.52919	78.19161	77.8524	77.51956	77.22322	76.94728	76.67
10	78.49693	78.16618	77.839035	77.49014	77.211784	76.927666	76.65
11	78.469864	78.14264	77.82136	77.486755	77.19062	76.909874	76.63
12	78.46088	78.13591	77.80325	77.47625	77.17676	76.891785	76.62
13	78.44167	78.11528	77.7804	77.46128	77.15831	76.87964	76.60
14	78.42656	78.09164	77.76545	77.439285	77.1513	76.85687	76.59
15	78.41652	78.06903	77.74367	77.42154	77.13272	76.84855	76.57
16	78.389755	78.05025	77.735405	77.421295	77.11447	76.83386	76.55
17	78.41643	78.06105	77.73454	77.40177	77.08778	76.820885	76.54
18	78.40275	78.03268	77.695305	77.37909	77.08377	76.79643	76.52
19	78.35617	78.008644	77.65941	77.37236	77.079346	76.78171	76.50
20	78.35407	77.98062	77.64952	77.36092	77.05212	76.769585	76.49
21	78.32391	77.962906	77.62076	77.333824	77.03806	76.75869	76.47
22	78.3192	77.953445	77.625244	77.30943	77.01282	76.73889	76.46

Appendix Table 1 Geolocation longitude


Latitude at /mod04/Geolocation Fields/ [MYD04_L2.A2013001.0840.006.2014078044830.psgscs_000500992112]

Table 

	0	1	2	3	4	5	6	7
0	30.110212	30.084656	30.06027	30.036896	30.013409	29.989923	29.966858	29.9442
1	30.19703	30.172304	30.148026	30.124739	30.100895	30.077671	30.054693	30.0321
2	30.287313	30.262318	30.238487	30.213902	30.190598	30.16759	30.144617	30.1220
3	30.374409	30.35017	30.325302	30.301016	30.278316	30.255297	30.232407	30.2099
4	30.463951	30.439346	30.41574	30.390472	30.3683	30.345179	30.322405	30.2999
5	30.54983	30.526115	30.502804	30.478333	30.455584	30.43301	30.410227	30.3878
6	30.638393	30.615604	30.591837	30.56791	30.54544	30.522635	30.499985	30.4777
7	30.724514	30.701832	30.67883	30.656145	30.632595	30.609367	30.587536	30.5656
8	30.814697	30.79039	30.769415	30.745281	30.721907	30.698658	30.676823	30.6555
9	30.901611	30.87716	30.85598	30.83358	30.810146	30.786263	30.764328	30.7433
10	30.991316	30.968197	30.944717	30.92279	30.90024	30.875187	30.854649	30.8330
11	31.079502	31.056736	31.031284	31.009665	30.98761	30.96372	30.941904	30.9206
12	31.169188	31.145006	31.12166	31.10024	31.077425	31.054127	31.032095	31.0104
13	31.256248	31.232025	31.208738	31.187307	31.164408	31.141771	31.119555	31.0985
14	31.346611	31.32195	31.298706	31.276718	31.254457	31.231327	31.210278	31.1880
15	31.43419	31.409746	31.386345	31.363602	31.341473	31.320248	31.297672	31.2763
16	31.524038	31.499508	31.47551	31.453327	31.431969	31.40986	31.387499	31.3664
17	31.611643	31.587109	31.565622	31.542551	31.52052	31.497156	31.474325	31.4543
18	31.702156	31.676498	31.655693	31.631664	31.608856	31.586683	31.565289	31.5438
19	31.789036	31.76484	31.74099	31.71852	31.694935	31.674942	31.653818	31.6316
20	31.878908	31.85558	31.831772	31.807602	31.785309	31.765247	31.74296	31.7219

Appendix Table 2 Geolocation Fields(latitude)

Corrected_Optical_Depth_Land_wav2p1 at /mod04/Data Fields/ [MYD04_L2.A2013001.0840.006.20140

Table 

	3	4	5	6	7	8	9
8	-9999	-9999	26	25	570	-9999	-9999
9	-9999	-9999	-9999	16	324	-9999	-9999
10	-9999	-9999	-9999	17	201	-9999	-9999
11	-9999	-9999	-9999	19	185	224	-9999
12	-9999	-9999	-9999	-9999	28	325	-9999
13	-9999	-9999	-9999	-9999	46	303	-9999
14	-9999	-9999	-9999	63	30	269	-9999
15	-9999	-9999	-9999	25	23	214	271
16	-9999	-9999	-9999	-9999	24	153	290
17	-9999	-9999	-9999	-9999	82	42	208
18	-9999	-9999	-9999	-9999	56	63	200
19	-9999	-9999	-9999	-9999	29	65	59
20	-9999	-9999	-9999	-9999	109	26	33
21	-9999	-9999	-9999	-9999	30	20	30
22	-9999	-9999	-9999	-9999	20	18	32
23	-9999	-9999	-9999	-9999	23	19	22
24	-9999	-9999	-9999	-9999	-9999	53	23
25	-9999	-9999	-9999	-9999	-9999	157	27
26	-9999	-9999	-9999	-9999	-9999	-9999	27
27	-9999	-9999	-9999	-9999	-9999	-9999	31
28	-9999	-9999	-9999	-9999	-9999	-9999	-9999
29	-9999	-9999	-9999	-9999	-9999	-9999	-9999
30	-9999	-9999	-9999	-9999	-9999	-9999	-9999

Appendix Table 3 Aerosol optical depth

APPENDIX-C

Sample daily data of RSPM/PM₁₀ HPPCB

Date	Monitoring agency	Station	6AM-2PM	2PM-10PM	10PM-2AM
05/01/2015	HPPCB	Tekka Bench	58.7	47.31	24.14
07/01/2015	HPPCB	Tekka Bench	37.87	85.65	67.15
09/01/2015	HPPCB	Tekka Bench	80.38	89.4	79.32
12/01/2015	HPPCB	Tekka Bench	77.77	86.24	73.31
16/1/2015	HPPCB	Tekka Bench	40.1	95.67	54.51
19/01/2015	HPPCB	Tekka Bench	40.17	33.18	43.05
21/01/2015	HPPCB	Tekka Bench	74.28	55.22	NA
23/01/2015	HPPCB	Tekka Bench	38.39	53.6	46.3
28/01/2015	HPPCB	Tekka Bench	47.45	49.53	37.71
30/01/2015	HPPCB	Tekka Bench	40.98	87.66	71.61
01/01/2015	HPPCB	Bus Stand	58.73	72.86	94.66
03/01/2015	HPPCB	Bus Stand	40.68	NA	NA
06/01/2015	HPPCB	Bus Stand	44.06	68.53	35.42
08/01/2015	HPPCB	Bus Stand	47.01	83.48	55.32
13/01/2015	HPPCB	Bus Stand	54.94	81.48	39.58
15/01/2015	HPPCB	Bus Stand	38.94	40.35	75.53
17/01/2015	HPPCB	Bus Stand	80.65	93.9	68.01
20/01/2015	HPPCB	Bus Stand	80.93	94.99	58.77
22/01/2015	HPPCB	Bus Stand	65.95	34.29	NA
24/01/2015	HPPCB	Bus Stand	73.55	87.95	NA
27/01/2015	HPPCB	Bus Stand	47.5	57.06	NA
29/01/2015	HPPCB	Bus Stand	87.76	88.79	101.63
31/01/2015	HPPCB	Bus Stand	119.95	80.5	87.2
02/02/2015	HPPCB	Tekka Bench	53.68	48.87	NA
04/02/2015	HPPCB	Tekka Bench	35.83	56.25	46.46
06/02/2015	HPPCB	Tekka Bench	58.85	57.05	37.53
09/02/2015	HPPCB	Tekka Bench	40.89	46.58	53.26
11/02/2015	HPPCB	Tekka Bench	51.52	43.53	43.78
13/02/2015	HPPCB	Tekka Bench	25.71	35.1	51.64
16/02/2015	HPPCB	Tekka Bench	31.4	41.47	NA
18/02/2015	HPPCB	Tekka Bench	21.48	39.09	36.44
23/02/2015	HPPCB	Tekka Bench	46.03	48.11	32.36
27/02/2015	HPPCB	Tekka Bench	43.86	43.08	46.23
05/02/2015	HPPCB	Bus Stand	68.76	79.49	61.66
07/02/2015	HPPCB	Bus Stand	71.42	69.13	79.9
10/02/2015	HPPCB	Bus Stand	74.44	70.33	84.8